

## Orthogonal Activation of the Reengineered A<sub>3</sub> Adenosine Receptor (Neoreceptor) Using Tailored Nucleoside Agonists

Zhan-Guo Gao,<sup>†</sup> Heng T. Duong,<sup>†</sup> Tatiana Sonina,<sup>‡</sup> Soo-Kyung Kim,<sup>†</sup> Philippe Van Rompaey,<sup>§</sup> Serge Van Calenbergh,<sup>§</sup> Liaman Mamedova,<sup>†</sup> Hea Ok Kim,<sup>||</sup> Myong Jung Kim,<sup>||</sup> Ae Yil Kim,<sup>||</sup> Bruce T. Liang,<sup>‡</sup> Lak Shin Jeong,<sup>\*,||</sup> and Kenneth A. Jacobson<sup>\*,†</sup>

Molecular Recognition Section, Laboratory of Bioorganic Chemistry, National Institute of Diabetes and Digestive and Kidney Diseases, National Institutes of Health, Bethesda, Maryland 20892, Department of Cardiology, University of Connecticut Health Center, Farmington, Connecticut 06030-1601, Laboratory for Medicinal Chemistry, Faculty of Pharmaceutical Sciences (FFW), Ghent University, Harelbekestraat 72, B-9000 Ghent, Belgium, and Laboratory of Medicinal Chemistry, College of Pharmacy, Ewha Womans University, Seoul 120-750, Korea

Received September 28, 2005

An alternative approach to overcome the inherent lack of specificity of conventional agonist therapy can be the reengineering of the GPCRs and their agonists. A reengineered receptor (neoreceptor) could be selectively activated by a modified agonist, but not by the endogenous agonist. Assisted by rhodopsin-based molecular modeling, we pinpointed mutations of the A<sub>3</sub> adenosine receptor (AR) for selective affinity enhancement following complementary modifications of adenosine. Ribose modifications examined included, at 3': amino, aminomethyl, azido, guanidino, ureido; and at 5': uronamido, azidodeoxy. N<sup>6</sup>-Variations included 3-iodobenzyl, 5-chloro-2-methoxybenzyl, and methyl. An N<sup>6</sup>-3-iodobenzyl-3'-ureido adenosine derivative **10** activated phospholipase C in COS-7 cells (EC<sub>50</sub> = 0.18 μM) or phospholipase D in chick primary cardiomyocytes, both mediated by a mutant (H272E), but not the wild-type, A<sub>3</sub>AR. The affinity enhancements for **10** and the corresponding 3'-acetamidomethyl analogue **6** were >100-fold and >20-fold, respectively. **10** concentration-dependently protected cardiomyocytes transfected with the neoreceptor against hypoxia. Unlike **10**, adenosine activated the wild-type A<sub>3</sub>AR (EC<sub>50</sub> of 1.0 μM), but had no effect on the H272E mutant A<sub>3</sub>AR (100 μM). Compound **10** was inactive at human A<sub>1</sub>, A<sub>2A</sub>, and A<sub>2B</sub>ARs. The orthogonal pair comprising an engineered receptor and a modified agonist should be useful for elucidating signaling pathways and could be therapeutically applied to diseases following organ-targeted delivery of the neoreceptor gene.

### Introduction

The approach of chemical genetics has been widely used to control various protein functions and cellular processes.<sup>1</sup> For example, this approach has been used in studying GTP regulatory proteins to create nucleotide specificity.<sup>2</sup> Gene-directed enzyme prodrug therapy has been proposed to be an effective means against cancer.<sup>3</sup> Tailor-made ligands for thyroid hormone nuclear receptors may have potential to restore mutation-caused genetic diseases.<sup>4</sup> It has been suggested that the chemical genetic approach is superior to the traditional genetic approach, such as gene knockout, in studying protein functions,<sup>5</sup> and has advantage for developing drugs against genetic diseases.<sup>6</sup> Functional orthogonal ligand–receptor pairs have been used for regulation of estrogen receptors,<sup>7,8</sup> Src family protein kinases,<sup>9</sup> and protein methyltransferases.<sup>10</sup>

In the GPCR field, engineering of orthogonal ligand–receptor pairs was initiated shortly after the cloning of the first non-rhodopsin GPCR.<sup>11,12</sup> The ligand binding domain of the β-adrenergic receptor has been genetically engineered to respond to specific classes of compounds which do not interact with the wild-type (WT) receptor. Targeting critical positions in the

ligand binding domains with specific functional groups on ligands was proposed to provide a novel avenue for design of therapeutic agents.<sup>12</sup> Indeed, the Gs-coupled β-adrenergic receptor–ligand pairs were further engineered and proposed for gene therapy, which should be therapeutically useful as they could potentially rescue the loss of function caused by SNPs (single nucleotide polymorphisms) which happened naturally at this receptor.<sup>13</sup> In the meantime, Coward et al.<sup>14</sup> by using a chimeric approach, engineered Gi-coupled κ-opioid receptors, and designated them as RASSLs (receptors solely activated by synthetic ligand). A RASSL showed dramatically decreased affinity for the endogenous agonist dynorphin and a wide range of other opioid peptides, but with a lesser extent of affinity decrease for the synthetic agonist spiradoline, and slowed heart rate in transgenic mice.<sup>14,15</sup> The RASSL approach is useful for unraveling the GPCR signaling mechanisms.<sup>14–19</sup> However, an ideal ligand–receptor pair for this purpose should be truly orthogonal, i.e., the endogenous agonist should not activate the engineered receptor and the synthetic ligand should not activate the wild-type receptor, and this goal has not actually been achieved. More recently, Bruysters et al.<sup>20</sup> engineered the Gq-coupled histamine H<sub>1</sub> receptor for enhanced affinity of a synthetic agonist, with decreased affinity for the endogenous agonist, but orthogonality was not complete.

Our initial work on engineering the receptors and ligands for orthogonal activation started with the A<sub>3</sub> adenosine receptor (AR),<sup>21</sup> the activation of which is both cerebro- and cardioprotective<sup>22,23</sup> and has an anticancer effect.<sup>24</sup> An integrated approach of engineering both ligands and receptors combined with molecular modeling was used. A H272E mutant receptor

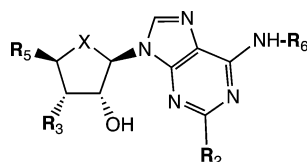
\* Corresponding authors: Dr. K. A. Jacobson, Chief, Molecular Recognition Section, Bldg. 8A, Rm. B1A-19, NIH, Bethesda, MD 20892-0810, Tel.: (301) 496-9024; Fax: (301) 480-8422; e-mail: kajacobs@helix.nih.gov and Lak Shin Jeong, Ph.D., Laboratory of Medicinal Chemistry, College of Pharmacy, Ewha Womans University, Seoul 120-750, Korea; Tel.: 82-2-3277-3466; Fax: 82-2-3277-2851; e-mail: lakjeong@ewha.ac.kr.

<sup>†</sup> National Institutes of Health.

<sup>‡</sup> University of Connecticut Health Center.

<sup>§</sup> Ghent University.

<sup>||</sup> Ewha Womans University.

**Table 1.** Affinities of Various 3'-Amine-Derivatized Adenosine Analogues in Binding Experiments at Wild-Type and H272E Mutant Human A<sub>3</sub>ARs. X = O and R<sub>2</sub> = H, Unless Noted<sup>a</sup>

	adenine substituent <sup>e</sup>		ribose substituents		K <sub>i</sub> (μM) or percentage inhibition at 10 μM		affinity enhancement
	R <sub>6</sub>	R <sub>3</sub>	R <sub>5</sub>	wild-type	H272E		
<b>1<sup>b</sup></b>	H	NH <sub>2</sub>	CH <sub>2</sub> OH	442 ± 121	75 ± 32	6-fold	
<b>2<sup>c</sup></b>	H	CH <sub>2</sub> NH <sub>2</sub>	CH <sub>2</sub> OH	3 ± 2%	2 ± 2%	NE	
<b>3<sup>b</sup></b>	H	NHC=NHNH <sub>2</sub>	CH <sub>2</sub> OH	130 ± 34	33.3 ± 7.1	4-fold	
<b>4<sup>b</sup></b>	IB	NH <sub>2</sub>	CH <sub>2</sub> OH	0.87 ± 0.18	0.32 ± 0.10	3-fold	
<b>5</b>	IB	CH <sub>2</sub> NH <sub>2</sub>	CONHCH <sub>3</sub>	0.137 ± 0.041	0.185 ± 0.027	NE	
<b>6</b>	IB	CH <sub>2</sub> NHCOCH <sub>3</sub>	CH <sub>2</sub> OH	15%	0.700 ± 0.099	>20-fold	
<b>7</b>	IB	CH <sub>2</sub> NH <sub>2</sub>	CH <sub>2</sub> OH	9.5 ± 1.7	0.61 ± 0.23	15-fold	
<b>8</b>	CMB	CH <sub>2</sub> NH <sub>2</sub>	CH <sub>2</sub> OH	13.8 ± 1.4	0.709 ± 0.163	20-fold	
<b>9</b>	CMB	CH <sub>2</sub> NH <sub>2</sub>	CONHCH <sub>3</sub>	0.557 ± 0.164	0.592 ± 0.081	NE	
<b>10<sup>d</sup></b>	IB	NHCONH <sub>2</sub>	CH <sub>2</sub> OH	9 ± 1%	0.22 ± 0.04	>100-fold	
<b>11</b>	IB, R <sub>2</sub> = Cl	NHCONH <sub>2</sub>	CH <sub>2</sub> OH	47 ± 9%	0.20 ± 0.03	~50-fold	
<b>12<sup>e</sup></b>	IB	NHCONH <sub>2</sub>	CONHCH <sub>3</sub>	5 ± 1%	2.7 ± 0.4	>10-fold	
<b>13</b>	Me	NHCONH <sub>2</sub>	CH <sub>2</sub> OH	3 ± 1%	30 ± 6%	NE	
<b>14<sup>e</sup></b>	Me	NHCONH <sub>2</sub>	CONHCH <sub>3</sub>	7 ± 2%	7 ± 1%	NE	
<b>15<sup>e</sup></b>	IB, X = O	N <sub>3</sub>	CONHCH <sub>3</sub>	2.26 ± 0.48	0.186 ± 0.034	12-fold	
<b>16</b>	IB, X = S	OH	CH <sub>2</sub> N <sub>3</sub>	0.022 ± 0.004	0.23 ± 0.04	NE	
<b>17</b>	H	OH	CONH-(CH <sub>2</sub> ) <sub>2</sub> NH <sub>2</sub>	>100	>100	NE	
<b>18<sup>f</sup></b>	H	OH	CONHNH <sub>2</sub>	1.5 ± 0.6	>10	NE	

<sup>a</sup> Binding parameters were measured in transiently transfected COS-7 cells as described in Experimental Procedures. The binding affinity was determined by using the agonist radioligand [<sup>125</sup>I]-AB-MECA (0.5 nM). Values represent the mean ± SE of at least three independent determinations. <sup>b</sup> Affinity at wild-type and mutant A<sub>3</sub>ARs previously reported.<sup>21</sup> <sup>c</sup> Affinity at wild-type A<sub>3</sub>AR stably expressed in CHO cells previously reported.<sup>37,38</sup> <sup>d</sup> MRS3481, LJ720. <sup>e</sup> IB = 3-iodobenzyl, CMB = 5-chloro-2-methoxybenzyl, Me = methyl, NE = no enhancement or insignificant enhancement. <sup>f</sup> MRS3412.

(designated as neoceptor) was found to have decreased affinity for classical ligands (20–50-fold), such as NECA (5'-N-ethylcarboxamidoadenosine) and Cl-IB-MECA (2-chloro-N<sup>6</sup>-(3-iodobenzyl)-5'-N-methylcarbamoyladenine), and with a modest affinity increase for a 3'-amine-derivatized adenosine (7-fold), but orthogonality has not been complete.<sup>21</sup> Further application of the neoceptor approach to 5'-uronamide derivatives that bound orthogonally at strategically mutated A<sub>2A</sub>ARs suggested that, in addition to the charge, the chain length of the interacting moiety (e.g., amine) was also critical for the affinity enhancement.<sup>25,26</sup> This observation was instructive for additional optimization of A<sub>3</sub> neoceptor-neoligand interactions.

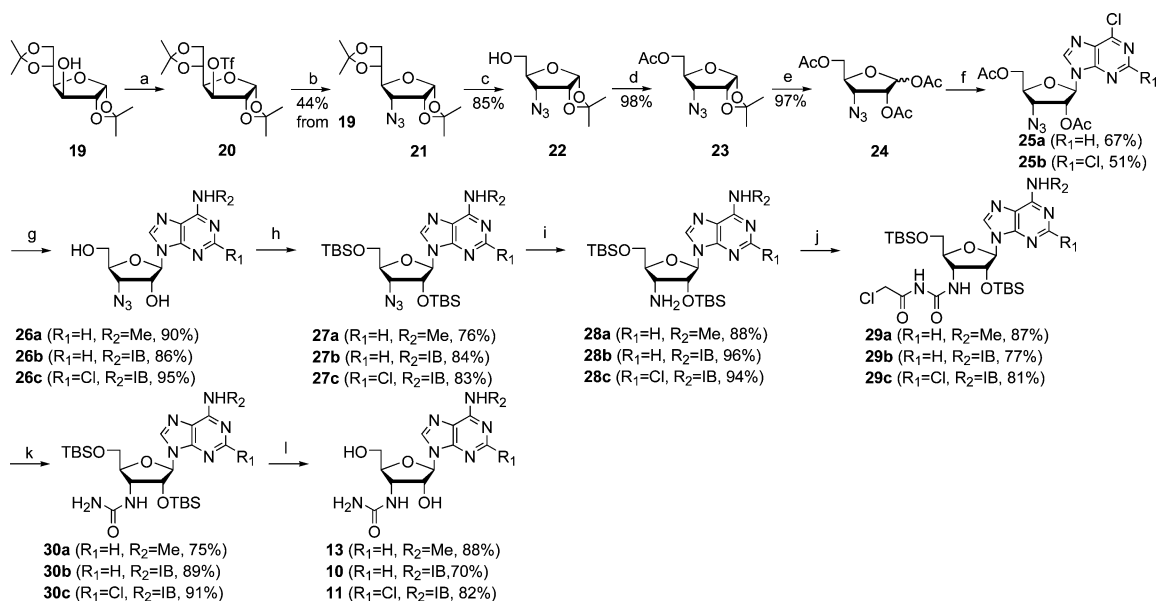
The neoceptor approach could be particularly suitable for application to ARs to achieve the receptor subtype-selectivity and tissue selectivity, which has proved difficult to achieve due to the ubiquitous presence of ARs. Here, with the assistance of molecular modeling, we systematically studied the interactions between the 3'-position of the nucleoside with negatively charged residues in place of the His residue. The charge, chain length, and H-bonding properties of the 3'-substitution were optimized in combination with substitutions at other positions of the adenosine molecule. We found that a derivative (**10**, N<sup>6</sup>-(3-iodobenzyl)-3'-ureidoadenosine) bearing both 3'-ureido and N<sup>6</sup>-3-iodobenzyl (IB) modifications displayed high selectivity for the H272E mutant receptor expressed in COS-7 cells in comparison to WT in binding and phospholipase C (PLC) assays. In contrast, the endogenous agonist adenosine (100 μM) had no effect at the H272E mutant receptor. The orthogonality of the neoceptor-neoagonist pair was functionally tested in a cardiomyocyte model showing activation of the cardioprotective phospholipase D (PLD) pathway and an antiischemic effect.<sup>27,28</sup> Additionally, it was found that, neither T94E nor Q167E, produced a similar pattern of affinity enhancement for a series of 3'-amine derivatized adenosine analogues. This selective gain of function, achieved by matching attractive substituents on the

ligand with those on the receptor at a specific site, could be explained by rhodopsin-based molecular modeling.

## Results

**Mutagenesis.** Single amino acid replacements of the hA<sub>3</sub>-AR were made at strategic locations of the putative ribose binding region, as defined by rhodopsin-based molecular modeling.<sup>31,35</sup> Thr94 (3.36) and His272 (7.43) were selected for mutation and individually replaced with Ala, Asp, or Glu. Both of these hydrophilic residues are predicted to be involved in coordination of the ribose moiety. The Gln167 residue of EL2, predicted to be in proximity to A<sub>3</sub>AR-bound nucleosides,<sup>36</sup> also served as a mutation site. His272, predicted to be in proximity to the 3'-OH group, was used successfully in the first study of neoceptors.<sup>21</sup>

**Nucleoside Structure.** A variety of adenine nucleoside derivatives (**1–18**, Table 1) were examined in this study as potential neoligands with respect to the above receptor mutations. Most of the modified adenosine derivatives were reported previously. Compounds **1**, **3**, **4**, **7**, **17**, and **18** were prepared as described.<sup>21,26</sup> The 3'-amino derivative **1** was identified previously as a suitable neoligand when paired with the H272E A<sub>3</sub>-AR neoceptor, although the degree of enhancement was low (Table 1). The 3'-aminomethyl derivatives **2** and **5–9** and 3'-azide **15** were reported recently.<sup>37</sup> The 3'-ureido moiety, found to result in inactivity the wild-type ARs, was included in analogues **10–14** and **16**.<sup>38,39</sup> Compounds **17** and **18** were identified previously as suitable neoligands when paired with A<sub>2A</sub>AR neoceptors.<sup>25,26</sup> The variations at the N<sup>6</sup>-position included unsubstituted, IB, 5-chloro-2-methoxybenzyl (CMB), and methyl. We previously reported that the CMB group increased affinity and selectivity at the human (h) A<sub>3</sub>AR in comparison to IB.<sup>36</sup> The 5'-position mainly consisted of either the ribose-like CH<sub>2</sub>OH or the NECA-like 5'-uronamide. To enhance selectivity for the hA<sub>3</sub>AR, the optimally substituted

Scheme 1<sup>a</sup>

<sup>a</sup> Reagents and conditions: (a) Tf<sub>2</sub>O, pyridine, 0 °C, 1 h; (b) NaN<sub>3</sub>, DMF, rt, 48 h; (c) (i) 75% AcOH, 55 °C, 1.5 h; (ii) NaIO<sub>4</sub>/H<sub>2</sub>O, EtOH, 0 °C, 20 min then NaBH<sub>4</sub>; (d) Ac<sub>2</sub>O, Pyridine, rt, 3 h; (e) (i) 85% HCO<sub>2</sub>H, 60 °C, 1.5 h; (ii) Ac<sub>2</sub>O, pyridine, rt, 16 h; (f) silylated 6-chloropurine or 2,6-dichloropurine, TMSOTf, C<sub>2</sub>H<sub>4</sub>Cl<sub>2</sub>, 0 °C to 60 °C, 2 h; (g) MeNH<sub>2</sub>, 1,4-dioxane, rt, 4 h or 3-iodobenzylamine hydrochloride, Et<sub>3</sub>N, EtOH, 50 °C, 18 h then NaOMe, MeOH, rt, 2 h; (h) TBSCl, imidazole, DMF, rt, 24 h; (i) Ph<sub>3</sub>P, NH<sub>4</sub>OH/H<sub>2</sub>O, THF, rt, 18 h; (j) chloroacetyl isocyanate, DMF, 0 °C, 3 h; (k) NaOMe, MeOH, rt, 18 h; (l) TBAF, THF, rt, 4 h. IB = 3-iodobenzyl.

5'-methyluronamide moiety was included. The 3'-position appeared to be the most critical for achieving selective affinity enhancement at neoreceptors derived from the hA<sub>3</sub>AR.<sup>21</sup> Thus, a variety of polar substituents (amino, guanidine, aminomethyl, acetamidomethyl, and ureido) were compared at this position. Only one compound, the 3'-ureido derivative **11**, was also substituted at the adenine 2-position.

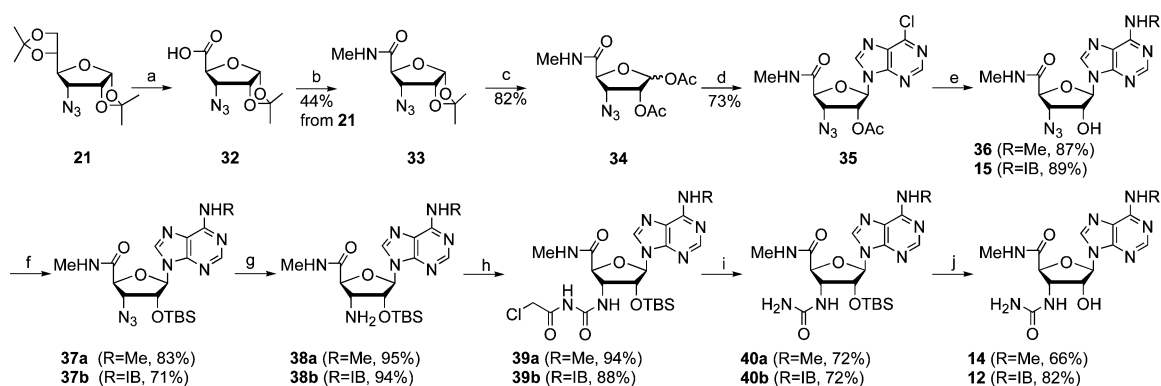
**Chemical Synthesis.** N<sup>6</sup>-Substituted-3'-ureidoadenosine derivatives **10**, **11**, and **13** were synthesized starting from 1,2:5,6-di-O-isopropylidene-D-glucose (**19**), as shown in Scheme 1. Reaction of **19** with triflic anhydride followed by treating the resulting triflate **20** with sodium azide afforded the 3-azido derivative **21**. Selective hydrolysis of the 5,6-isopropylidene group of **21** followed by oxidative cleavage and reduction gave **22** in 85% yield. Treatment of **22** with acetic anhydride gave **23** which was converted to the glycosyl donor **24** in two steps (hydrolysis and acetylation). Condensation of **24** with silylated 6-chloropurine and 2,6-dichloropurine in the presence of TMSOTf afforded the protected nucleosides **25a** and **25b**, respectively. 6-Chloropurine derivative **25a** was treated with methylamine and 3-iodobenzylamine followed by treating with sodium methoxide to give the N<sup>6</sup>-methyl derivative **26a** and N<sup>6</sup>-3-iodobenzyl derivative **26b**, respectively. 2,6-Dichloropurine derivative **25b** was also converted to 2-chloro-N<sup>6</sup>-3-iodobenzyl derivative **26c**. Compounds **26a–c** were reprotected as TBS-ethers **27a–c**, respectively. The reason that the acetyl protecting groups were replaced with TBS protecting groups was because of the facile migration of a 2'-acetyl group to the 3'-ureido group. Reduction of the azido group of **27a–c** using triphenylphosphine and ammonium hydroxide in aqueous solution yielded amino derivatives, **28a–c**, respectively. For the conversion of 3'-amino group into a 3'-ureido group, the 3'-amino derivatives **28a–c** were treated with chloroacetyl isocyanate in DMF to yield 3'-chloroacetyl urea derivatives **29a–c**, which were smoothly converted to the 3'-ureido derivatives **30a–c**, respectively, after treating with sodium methoxide. As mentioned above, migration of a 2'-acetyl or benzoyl group to the 3'-ureido group was observed upon treating the 3'-chloroacetyl

urea derivatives with sodium methoxide, giving an N-acetyl- or N-benzoylureido derivative as a sole product. This migration was prevented by using a TBS group as a protecting group. Removal of the TBS group of **30a–c** with TBAF in THF afforded the final N<sup>6</sup>-substituted-3'-ureidoadenosine derivatives **13**, **10**, and **11**, respectively.

N<sup>6</sup>-Substituted-3'-ureidoadenosine-5'-methyluronamides **14** and **12** were also synthesized starting from the same intermediate **21**, as illustrated in Scheme 2.<sup>38</sup> Selective hydrolysis of the 5,6-isopropylidene group of **21** using 75% aqueous acetic acid followed by treatment of the resulting diol with NaIO<sub>4</sub>/RuCl<sub>3</sub> in CCl<sub>4</sub>/CH<sub>3</sub>CN/H<sub>2</sub>O (2/2/3) produced acid derivative **32**. Treatment of **32** with oxalyl chloride gave the activated ester, which was converted to methyl amide **33** by treating with methylamine. Compound **33** was converted to the key intermediate **34** using the same conditions described in Scheme 1. The key intermediate **34** was transformed to the final nucleosides **12** and **14** according to the same procedure used in the preparation of **10**, **11**, and **13** in Scheme 1.

**Ligand Binding Properties at the Wild-Type and Mutant Receptors.** The affinities of the nucleoside derivatives were initially evaluated at wild-type and H272E mutant A<sub>3</sub>ARs expressed in COS-7 cells (Table 1). Only the substituted N<sup>6</sup>-benzyl derivatives **4**, **5**, **9**, and **16** displayed a K<sub>i</sub> value at the wild-type A<sub>3</sub>AR of <1 μM.<sup>26,38</sup> All of the other compounds were weak or inactive at all four subtypes of ARs.<sup>37,38</sup>

Adenosine bound to the wild-type A<sub>3</sub>AR with a K<sub>i</sub> value of 1 μM, while at the mutant H272E A<sub>3</sub>AR adenosine at 100 μM failed to inhibit radioligand binding (Figure 1). Considerable enhancement of affinity was observed for several nucleoside analogues. Following the introduction of a carboxylic acid side chain at position 7.43, the 3'-acetamidomethyl derivative **6** and the 3'-aminomethyl derivatives **7** and **8** were 10- to 20-fold enhanced in affinity. The enhancement of the 3'-aminomethyl derivatives was dependent on the presence of an N<sup>6</sup>-benzyl-type group (either IB in **7** or CMB in **8**). The corresponding simple 6-NH<sub>2</sub> derivative **2** was not enhanced in affinity. The greatest degree of enhancement (>100-fold) was observed for

Scheme 2<sup>a</sup>

<sup>a</sup> Reagents and conditions: (a) (i) 75% AcOH, 55 °C, 1.5 h; (ii) NaIO<sub>4</sub>, RuCl<sub>3</sub>·H<sub>2</sub>O, CCl<sub>4</sub>/CH<sub>3</sub>CN/H<sub>2</sub>O, rt, 4 h; (b) (i) (COCl)<sub>2</sub>, DMF, CH<sub>2</sub>Cl<sub>2</sub>, rt, 16 h; (ii) 2 M NH<sub>2</sub>CH<sub>3</sub>, CH<sub>2</sub>Cl<sub>2</sub>, 0 °C, 3 h; (c) AcOH/Ac<sub>2</sub>O/concd H<sub>2</sub>SO<sub>4</sub>, rt, 16 h; (d) silylated 6-chloropurine, TMSOTf, C<sub>2</sub>H<sub>4</sub>Cl<sub>2</sub>, 0 °C to 60 °C, 2 h; (e) MeNH<sub>2</sub>, 1,4-dioxane, rt, 4 h or 3-iodobenzylamine hydrochloride, Et<sub>3</sub>N, EtOH, 50 °C, 18 h then NaOMe, MeOH, rt, 2 h; (f) TBSCl, imidazole, DMF, rt, 24 h; (g) Ph<sub>3</sub>P, NH<sub>4</sub>OH/H<sub>2</sub>O, THF, rt, 18 h; (h) chloroacetyl isocyanate, DMF, 0 °C, 3 h; (i) NaOMe, MeOH, rt, 18 h; (j) TBAF, THF, rt, 4 h or Et<sub>3</sub>N·3HF, THF, 50 °C, 16 h. IB = 3-iodobenzyl.

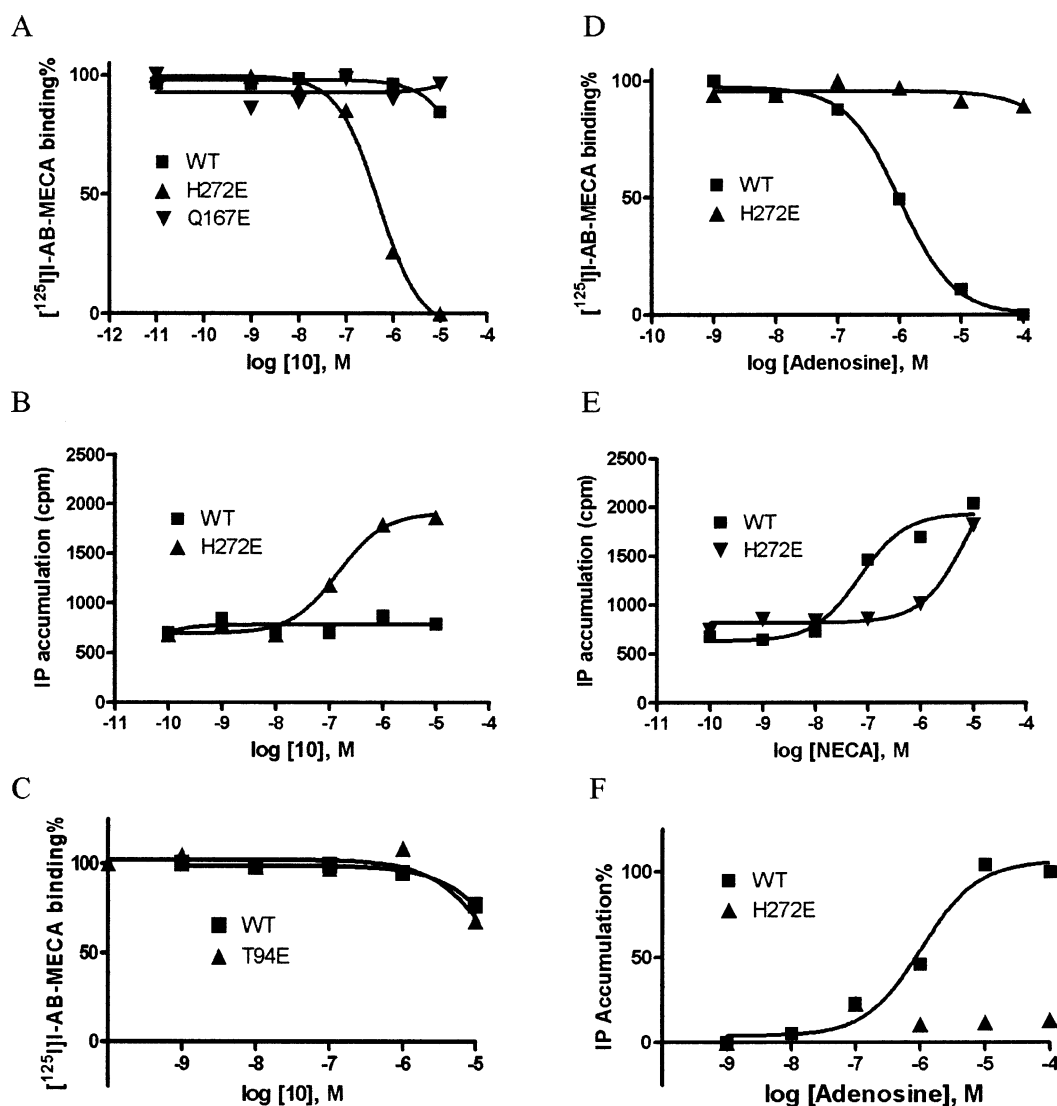


**Figure 1.** Binding inhibition and functional activation in wild-type and H272E mutant A<sub>3</sub>ARs. The receptors were expressed transiently in COS-7 cells as described in Experimental Procedures. The binding affinity ( $K_i$ ) was determined by using the agonist radioligand [125I]-AB-MECA (0.5 nM). The structure of compound 10 is given in Table 1.

the 3'-ureido derivative 10 (Figure 1A), which also contained the IB group. The corresponding 2-Cl analogue 11 showed an approximately 50-fold affinity increase. Compounds 15 and 16

both had azido groups on the ribose moiety, while only the 3'-azido derivative 15, not 5'-azido derivative 16, displayed enhanced affinity at the H272E mutant A<sub>3</sub>AR, further supporting

**Table 2.** Comparison of the Effects of 3'-Aminomethyl- and 3'-Ureido-derivatized Adenosine Analogues in Binding Experiments at Wild-Type and Mutant Human A<sub>3</sub>ARs<sup>a</sup>

compound	K <sub>i</sub> values (μM) <sup>b</sup>					
	wild-type	T94A	T94E	H272D	H272E	Q167E
<b>5</b>	0.14 ± 0.04	0.12 ± 0.01	0.11 ± 0.05	0.12 ± 0.03	0.18 ± 0.03	0.57
<b>6</b>	>10	>10	>10	1.0 ± 0.3	0.70 ± 0.10	>10
<b>7</b>	9.5 ± 1.7	10.7 ± 2.9	10.0 ± 1.4	0.85 ± 0.12	0.61 ± 0.23	>10
<b>8</b>	13.8 ± 1.4	9.8 ± 4.2	>10	2.0 ± 0.4	0.71 ± 0.16	>10
<b>9</b>	0.56 ± 0.16	ND	0.85 ± 0.19	0.39 ± 0.20	0.59 ± 0.08	7.2
<b>10</b>	>10	>10	>10	0.47 ± 0.07	0.22 ± 0.04	>100
<b>15</b>	2.26 ± 0.48	1.37 ± 0.13	2.0 ± 0.1	0.14 ± 0.00	0.19 ± 0.03	ND <sup>b</sup>

<sup>a</sup> Binding parameters (K<sub>i</sub> values) were measured in transiently transfected COS-7 cells as described in Experimental Procedures by using the agonist radioligand [<sup>125</sup>I]-AB-MECA (0.5 nM). The K<sub>d</sub> values for the WT, T94E, and T94A mutant were determined to be 1.8 ± 0.8, 2.0 ± 0.1, and 2.6 ± 1.2 nM, respectively, while over 10 nM for other mutants. Values represent the mean ± SE of at least three independent determinations. <sup>b</sup> The H272A mutant receptor lost high-affinity binding to both agonist and antagonist radioligands; therefore, competitive binding experiments could not be performed. <sup>c</sup> ND = not determined.

a specific interaction between the 3'-position and His272E. Two other 5'-substituted derivatives, **17** and **18**, also did not show any enhancement at the H272E neoreceptor.

The affinity enhancement at the neoreceptors, for nucleosides substituted at the 3'-position with amino, aminomethyl, and ureido moieties, was greatly attenuated when a 5'-uronamide group was also present, i.e., **5**, **9**, and **12**. Although the affinity at the wild-type A<sub>3</sub>AR was increased by this structural change—for example, by 22-fold in the case of 5'-methyluronamide **9**—there was no affinity enhancement at the H272E mutant receptor, as was observed for the corresponding **8**. The affinity of 5'-methyluronamide **12** was decreased in comparison to the corresponding 5'-OH derivative **10** at the H272E mutant A<sub>3</sub>AR.

Table 2 shows a comparison of affinities of selected nucleosides at various mutant A<sub>3</sub>ARs. Negatively charged side chains were introduced at positions 3.36 and 7.43. Thr94 (3.36) is analogous to Thr88 of the hA<sub>2A</sub>AR, which was the site of mutagenesis used successfully to construct neoreceptors of that subtype.<sup>26</sup> The Gln167 residue of EL2, predicted to be in proximity to A<sub>3</sub>AR-bound nucleosides,<sup>36</sup> also served as a mutation site. However, no enhancement of affinity of any modified nucleoside in the present study was observed at T94A, T94E, and Q167E mutant receptors. The affinity at the H272D mutant receptor closely paralleled the affinity at the H272E mutant receptor. This indicates that there is sufficient steric freedom within the binding site to preserve the effect after adding or subtracting one methylene unit. The T94A and T94E mutant receptors were similar to wild-type.

Binding experiments were carried out at human A<sub>1</sub> and A<sub>2A</sub>-ARs expressed in CHO (Chinese hamster ovary) cells using standard radioligand binding assays, as described.<sup>37</sup> Compounds **1–3**, **5–9**, and **15** were previously determined to have K<sub>i</sub> values >1 μM at the A<sub>1</sub>AR and >10 μM at the A<sub>2A</sub>AR.<sup>37</sup> Compound **4** was previously determined to have K<sub>i</sub> values of 8.1 μM and 28 μM at the rat A<sub>1</sub> and A<sub>2A</sub>ARs, respectively.<sup>21</sup> 3'-Ureido derivatives **10–14** were assayed in binding to human A<sub>1</sub> and A<sub>2A</sub>ARs. In all cases, <10% inhibition of binding was observed at 10 μM, except for **11** at the A<sub>1</sub>AR (34% inhibition). Thus, all of the nucleosides that displayed affinity enhancement at the H272E mutant receptor only weakly bound, if at all, to two other AR subtypes. Compound **10** at 10 μM was inactive in the stimulation of cyclic AMP formation mediated by the human A<sub>2B</sub>AR expressed in CHO cells.<sup>36</sup>

**Functional Effects of Nucleosides at WT and Mutant A<sub>3</sub>ARs.** An assay of PLC was used in the determination of functional coupling of the WT and mutant A<sub>3</sub>ARs expressed in COS-7 cells in response to known AR agonists and modified nucleosides. As illustrated in Figure 1B, **10** induced accumulation of inositol phosphates in COS-7 cells expressing the H272E

mutant receptor with an EC<sub>50</sub> of 0.18 ± 0.098 μM (*n* = 3), while it had no effect on the WT ARs at concentrations as high as 10 μM. In contrast, the known agonist NECA (Figure 1E) activated the WT A<sub>3</sub>AR with an EC<sub>50</sub> of 0.078 ± 0.020 μM (*n* = 3), and H272E with an EC<sub>50</sub> of 10.4 ± 3.3 μM (*n* = 3). Similar to the loss of affinity for NECA, the endogenous agonist, adenosine, activated the WT ARs with an EC<sub>50</sub> of 1.04 μM while it had no effect on the H272E mutant receptor at 100 μM (Figure 1F). No enhancement in basal PLC activity was observed for the mutant receptor in the absence of nucleoside. A 3'-azido substituted derivative **15**, and a 5'-azido derivative **16**, failed to activate PLC in either the wild-type A<sub>3</sub>AR or the H272E neoreceptor (data not shown). The functional effects of other derivatives at the WT A<sub>3</sub>AR expressed in CHO cells were probed previously.<sup>37</sup>

**Cardiomyocyte Model.** In a known model of cardioprotection from 90 min of simulated ischemia,<sup>27,28,33,40</sup> endogenous adenosine significantly protected cardiomyocytes transfected with the hA<sub>3</sub>AR (10 ± 7% cells killed in hA<sub>3</sub>AR-transfected cells, *n* = 9, compared with 28 ± 6.5%, *n* = 8, in vector-transfected overexpressing myocytes; one-way ANOVA, *F* = 14.7, *P* < 0.0001, followed by posttest comparison, *P* < 0.001). Unlike the wild-type A<sub>3</sub>AR, cells expressing the neoreceptor H272E cDNA only showed a slight change. In cells expressing the H272E mutant receptor, the neoligand **10** induced potent cardioprotection against hypoxia and activated the known cardioprotective PLD pathway (Figure 2). Adenosine (100 μM) did not activate the PLD pathway in myocytes expressing the H272E mutant receptor.

**Molecular Modeling and Nucleoside Docking.** Recently a hA<sub>3</sub>AR model, including the seven TMs and loop regions, was constructed<sup>31,41,42</sup> by homology to the X-ray structure of bovine rhodopsin.<sup>35</sup>

For the side-chain refinement of the neoreceptors, the H272E mutant receptor was optimized through a molecular dynamics procedure after the mutation of His to Glu. In the WT A<sub>3</sub>AR, there was a TM H-bonding network between the highly conserved His272 (7.43) and Glu19 (1.39), as previously described.<sup>21</sup> The mutant H272E hA<sub>3</sub>AR showed the same preference of the side-chain χ<sub>1</sub> angle at position 7.43 as did WT, but it had a different intramolecular H-bonding pattern. The H272E mutant receptor lost H-bonding between position 7.43 and Glu19, due to the electronic repulsion between two ionized Glu side chains, showing a distance of 4.88 Å between two C<sub>δ</sub> atoms of Glu19 and Glu272.

A conformational search of the isolated 3'-ureido derivative **10**, carried out with a MOPAC PM3 calculation,<sup>43</sup> showed that the lowest-energy conformer displayed intramolecular H-bonding between the 3'-carbonyl oxygen of the ureido group and

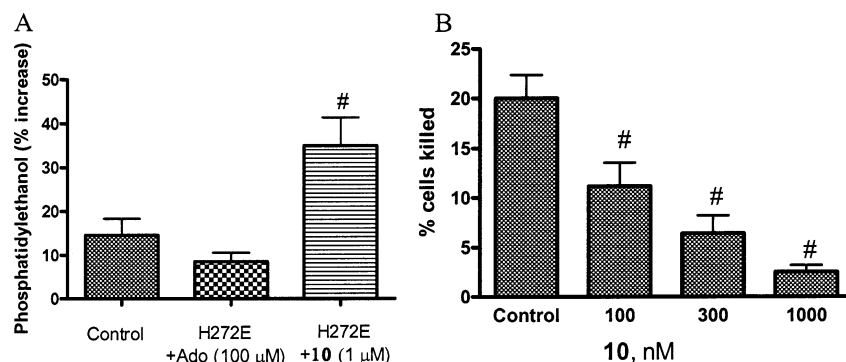


**Figure 2.** Activation of the neoreceptor by the neogonist **10** protects heart cells from ischemia-induced injury. A) Activation of PLD by **10** in chick cardiomyocytes expressing the mutant human H272E A<sub>3</sub>AR. B) Effect of **10** on antiischemic cardioprotection in neoreceptor-transfected cardiac myocytes is shown. Cardiac ventricular myocytes were transfected with cDNA encoding the neoreceptor H272E, and the percentage of cells killed was determined in the absence or the presence of **10** during the 90-min simulated ischemia, as described in Experimental Procedures. Data were plotted as the percentage of cells killed during the prolonged simulated ischemia. #*P* < 0.01 compared with control (ANOVA). ANOVA (all four groups), *F* = 15.6, *P* < 0.0001; all posttest comparisons were significant at *P* < 0.01 except for the percentage of cells killed at 300 nM **10** compared with 1000 nM and that for 100 nM compared with 300 nM.

the 5'-hydroxyl group and between the 3'-amino and 2'-hydroxyl groups. The lowest-energy conformer of **12**, having a 5'-uronamide, formed H-bonding between the 3'-CO and 2'-OH groups and between the 5'-NH and the O of the ribose ring. However, this conformer of **12** showed no interaction between 3'- and 5'-substituents. Thus, the thermodynamic stability of the various intramolecular H-bonds, depending on the substitution pattern, might affect the binding affinity.

A complex of the A<sub>3</sub>-selective agonist Cl-IB-MECA docked in the hA<sub>3</sub>AR was constructed with only minor modifications from the previous model.<sup>31,41</sup> This model featured putative H-bonds between the exocyclic NH and the side chain nitrogen (lone pair) of N250 (6.55) and between the carboxamide NH of Gln167 (EL2) and the purine N<sup>3</sup> atom. This docked ligand showed an anti-conformation of the adenine ring. In the putative binding site of the ribose ring, intermolecular H-bonds formed between the 2'-OH group and the carbonyl O atom of Ile268 (7.39) and among the 3'-OH group, the backbone O of Ser271 (7.42), and the imidazole ring of His272 (7.43). The 5'-amide NH also formed a H-bond with Thr94 (3.36), and the 5'-carbonyl group displayed intramolecular H-bonding with the 3'-hydroxyl group. However, the docked conformation of N<sup>6</sup>-methyl-3'-ureidoadenosine **14**<sup>38</sup> showed no H-bonding interaction of the 3'- and 5'-substituents with Ser271 or His272, consistent with its loss of binding affinity at all subtypes of ARs. The lack of H-bonding was expected from the observed electronic and steric repulsion of the starting geometry of 3'-ureidoadenosine derivatives.<sup>38</sup>

While these 3'-ureidoadenosine analogues lost binding affinity at all subtypes of ARs, they exhibited highly selective enhancement of binding affinity at the H272D or H272E mutant A<sub>3</sub>-ARs, suggesting a favorable interaction between 3'-ureido group and mutated acidic residues. While Cl-IB-MECA, a selective A<sub>3</sub> agonist, displayed a single favorable binding mode, the docking result of the 3'-ureido analogue **10** from the combination of the FlexiDock and FlexX<sup>57</sup> automatic docking programs had two energetically favorable binding modes. The docking results showing two putative complexes of the hA<sub>3</sub> H272E AR with compound **10** are shown in Figure 3. As illustrated in Figure 3A, one binding mode similar to that of Cl-IB-MECA, gained energetically through H-bonding of the 3'-ureido substituent and of the 2'-hydroxyl group with the  $\gamma$ -carboxylate group of Glu272 (7.43), but lost hydrophilic interactions, i.e., H-bonding, at the N<sup>6</sup> and the N<sup>3</sup> atoms in the adenine ring. According to the model, the oxygens of the Glu272 side chain were each H-bonded to

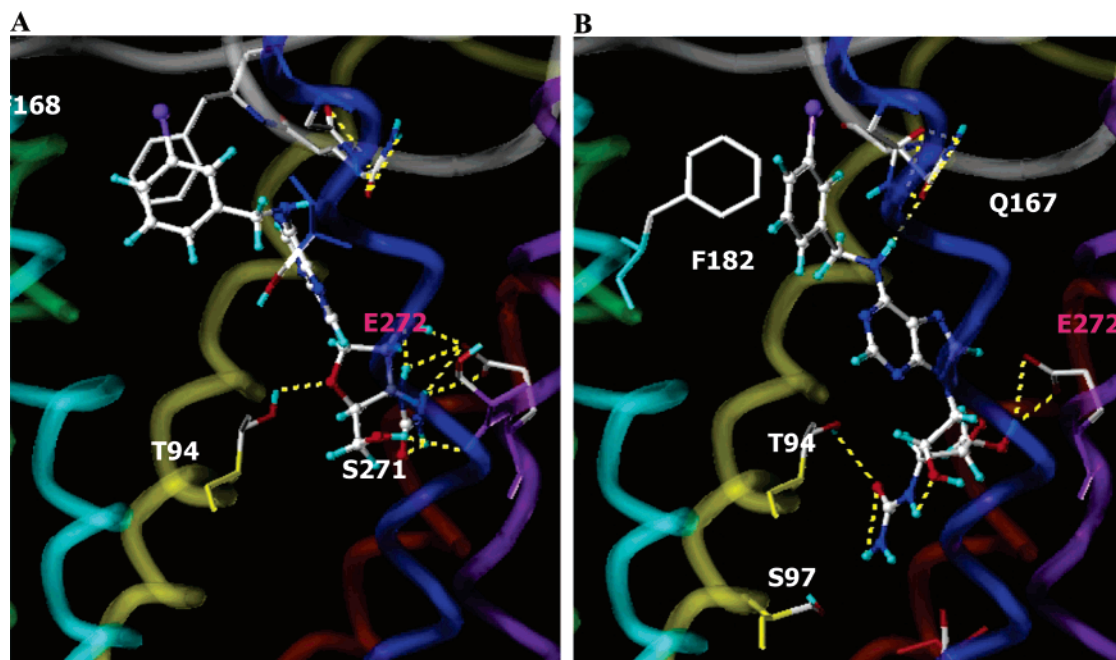
one of the urea NH groups in a bidentate fashion. The 5'-hydroxyl group H-bonded with the backbone O atom of Ser271 (7.42).

Figure 3B shows another possible binding mode, in which the 3'-ureido group interacted with the Thr94 (3.36) side chain through H-bonding and the 5'-hydroxyl group formed a H-bond with the carboxylate group of Glu272 (7.43) and the terminal 3'-NH<sub>2</sub> group was close to Ser97 (3.39). The N<sup>6</sup>-amino group interacted through H-bonding with Gln167 (EL2), a residue previously predicted to be in proximity to the nucleoside.<sup>36</sup> In comparison to Figure 3A, this docking mode required a different orientation of the N<sup>6</sup>-benzyl ring toward Phe182 (5.43). Molecular modeling indicates that the reason for the enhanced binding affinity of N<sup>6</sup>-benzyl compared with N<sup>6</sup>-methyl derivatives may be additional hydrophobic interaction at the N<sup>6</sup>-benzyl group.

## Discussion

In this study, we used an integrated approach of mutagenesis, radioligand binding and functional assays combined with molecular modeling to identify matched pairs of neoligands and neoreceptors. We tested a wide range of synthetic amine-bearing nucleoside analogues and modulated the 3'-substituent chain length in concert with N<sup>6</sup>-, 5'-, and 2'-modifications to identify engineered agonists that orthogonally activate mutant but not wild-type receptors. Mutation of His272, to Ala, Asp, and Glu, was compared with the WT A<sub>3</sub>AR to optimize the electrostatic or H-bonding interaction between the 3'-amino moiety and the carboxylate group of the mutation site. The extended and multiply H-bonding 3'-deoxy-3'-ureido derivative **10**, containing an N<sup>6</sup>-3-iodobenzyl substituent, had no significant effect on the wild-type A<sub>3</sub>AR but displayed a dramatically enhanced affinity of 0.22  $\mu$ M at the H272E neoreceptor. In a previous study,<sup>21</sup> it was demonstrated that the H272E neoreceptor showed decreased affinity for NECA and Cl-IB-MECA, here we further demonstrated this neoreceptor is completely insensitive to the endogenous agonist, adenosine, as demonstrated in both binding and functional assays. Thus, truly orthogonal ligand-receptor pairs have been identified, which should be useful in elucidating signaling transduction mechanisms and should provide insights into the therapeutics of genetically related diseases.

Mutations in genes encoding G protein-coupled receptors (GPCRs) are an important cause of human disease.<sup>44</sup> Study of the high-resolution SNP maps of 23 genes encoding GPCRs in the Japanese population identified 300 SNPs, including 83 in



**Figure 3.** Two energetically favorable binding modes of the *N*<sup>6</sup>-(3-*I*-benzyl)-3'-ureidoadenosine **10** in the binding site of the mutant H272E hA<sub>3</sub>-AR. The binding mode similar to the hA<sub>3</sub>/Cl-IB-MECA complex (A) and another binding mode (B), which was energetically unfavorable in the hA<sub>3</sub>/Cl-IB-MECA complex, are shown. All ligands are displayed as ball-and-stick models in the atom-by-atom color, and the side chains of the hA<sub>3</sub>AR are shown as stick models. The H-bonding between each ligand and the mutant hA<sub>3</sub>AR is displayed in yellow. The A<sub>3</sub>AR is represented by a tube model with a different color for each TM (TM2 in orange, TM3 in yellow, TM4 in green, TM5 in cyan, TM6 in blue, TM7 in purple).

adenosine receptor family genes.<sup>45</sup> The A<sub>2A</sub> adenosine receptor 1976T>C genetic variant has been shown to confer susceptibility to panic disorder and caffeine-induced anxiety.<sup>46,47</sup> Specific GPCR polymorphisms in adrenergic genes have already been shown to confer susceptibility to congestive heart failure.<sup>13</sup> Development of small molecules for GPCRs to rescue mutation induced functional loss or to inhibit mutation-caused constitutive activation will be novel forms of treatment for such diseases.

The reengineering of the interface of small molecules and proteins, such that the mutated protein will interact exclusively with chemically modified ligand in an orthogonal manner, has been explored for a variety of targets including receptors, enzymes, etc., to elucidate the role of signal transduction pathways in living systems.<sup>48–51</sup> The neoceptor approach, which focuses on cell-surface GPCRs, is intended for therapeutic application that employs a targeted vector to deliver the neoceptor gene to a target organ. In addition to the potential therapeutic applications, the neoceptor/neoligand pairs may be used for specific mechanistic probing of pharmacological effects, for example, in cases where the application of a normal receptor agonist might cause complicating effects. In several aspects, the neoceptor approach described in this study may be distinguished from the RASSL approach as described.<sup>14</sup> First, the neoceptor approach concerns the reengineering of both the receptor and the ligands using molecular modeling. Second, the RASSL described earlier<sup>14</sup> showed somewhat parallel affinity decrease for both endogenous and synthetic ligands, which is not truly orthogonal. The synthetic agonist may activate the endogenous receptor and the engineered receptor simultaneously. Third, the RASSL was achieved by engineering a chimeric receptor, while the neoceptor is achieved by reengineering the TM binding site for a specific group of the small-molecule agonist as predicted by using molecular modeling.

The neoceptor approach could be particularly useful for studying ARs to achieve the receptor-subtype-selectivity and tissue selectivity due to the ubiquitous presence of ARs.<sup>52</sup> In the present study, the functionality of the neoagonist/neoceptor

concept was further tested in a cardiac myocyte model of simulated ischemia and cardioprotection. Cardiomyocytes overexpressing the wild-type hA<sub>3</sub>AR, activated by endogenous adenosine released by ischemia, showed potent antiischemic resistance. In contrast, cells expressing the H272E mutant receptor showed only a slight change. Activation of the overexpressed neoceptor by the neoligand resulted in a full antiischemic protective effect. The demonstration that the neoligand was able to induce a potent activation of the cardioprotective PLD pathway<sup>27,28</sup> provides additional support for this concept.

We used site-directed mutagenesis to probe the recognition elements responsible for the selective affinity enhancement. The neoligand **10** was found to bind with higher affinity to carboxylic acid mutations at a spatially distinct region of the A<sub>3</sub>AR, i.e., receptors containing H272E (or D) in TM7 mutations, expressed in COS-7 cells, while other mutations (T94A, T94E or Q167E in EL2) did not result in this gain in affinity. This was consistent with the docking mode of **10** that was similar to that of the high affinity agonist Cl-IB-MECA (Figure 3A), but not the alternate binding mode (Figure 3B).

A carboxylic acid introduced in the sequence of the human A<sub>3</sub>AR was found to pair with several functional groups on the ligand in an energetically favorable manner. Pairing of an Asp or Glu residue with an amino or aminomethyl group could be explained on the basis of an electrostatic attraction. The enhancement of the 3'-azido derivative **15** may also result from an electrostatic interaction with the middle nitrogen of the N<sub>3</sub> group, which would be positively charged. Finally, the successful pairing of a 3'-ureido group with the carboxylate could be explained on the basis of the ability of both groups to form multiple H-bonds.

## Conclusions

We have identified an engineered agonist that activates exclusively neoceptors and have shown that the orthogonality

of binding and activation results in cardioprotective effects. This suggests that the 3'-urea derivatives described in this study might be useful therapeutically in combination with targeted gene delivery of a carboxylic acid mutant A<sub>3</sub>AR such as H272E. The neoceptor, in general, could be an important therapeutic approach for tissue-specific GPCR activation, given successful targeted delivery (without side effects) of the neoceptor gene to a specific organ or tissue.

## Experimental Procedures

**Chemical Synthesis. General.** <sup>1</sup>H NMR spectra were recorded in a 300 MHz apparatus using tetramethylsilane (TMS) as an internal standard, and the chemical shifts are reported in ppm (δ). Coupling constants are reported in Hertz (Hz). Optical rotations were determined on Jasco III in methanol of DMF. Infrared spectra were recorded in a Perkin-Elmer 1710 FTIR spectrophotometer. Mass spectra recorded by FAB (Fast atom bombardment) on a VG Tro-2, GC-MS. TLC were carried out on Merck silica gel 60 F<sub>254</sub> precoated plates, and silica gel column chromatography was performed on silica gel 60, 230–400 mesh, Merck. All anhydrous solvents were distilled over CaH<sub>2</sub> or Na/benzophenone prior to use.

**3-Azido-3-deoxy-1,2;5,6-di-*O*-isopropylidene- $\alpha$ -D-allofuranose (21).** To a stirred solution of 1,2;5,6-di-*O*-isopropylidene- $\alpha$ -D-glucofuranose (3.0 g, 11.53 mmol) and pyridine (2.8 mL, 34.62 mmol) in dichloromethane (30 mL) was added trifluoromethanesulfonic anhydride (2.9 mL, 17.24 mmol) at 0 °C. After being stirred for 1 h at 0 °C, the reaction mixture was extracted with dichloromethane and water. The organic layer was washed with brine, dried (MgSO<sub>4</sub>), filtered, and evaporated to give **20**.

To a solution of **20** in anhydrous DMF (20 mL) was added sodium azide (2.25 g, 34.61 mmol), and the mixture was stirred at room temperature for 48 h. The reaction mixture was poured into water (200 mL) and extracted with ethyl acetate ( $\times$  3). The combined organic layers were dried (MgSO<sub>4</sub>), filtered, and evaporated. The residue was purified by silica gel column chromatography (hexanes/EtOAc = 4/1) to give **21** (1.45 g, 44%) as an oil: <sup>1</sup>H NMR (CDCl<sub>3</sub>) δ 5.76 (d, 1 H, *J* = 3.7 Hz), 4.70 (t, 1 H, *J* = 4.1 Hz), 3.95–4.21 (m, 4 H), 3.48 (dd, 1 H, *J* = 4.9, 9.0 Hz), 1.56 (s, 3 H), 1.46 (s, 3 H), 1.36 (s, 3 H), 1.34 (s, 3 H); IR (KBr): 2109 (N<sub>3</sub>) cm<sup>-1</sup>; FAB-MS *m/z* 286 [M + H]<sup>+</sup>. Anal. (C<sub>12</sub>H<sub>19</sub>N<sub>3</sub>O<sub>5</sub>) C, H, N.

**3-Azido-3-deoxy-1,2-*O*-isopropylidene- $\alpha$ -D-ribofuranose (22).** A mixture of **21** (2.63 g, 9.22 mmol) in 75% AcOH (30 mL) was stirred at 55 °C for 1.5 h. The reaction mixture was evaporated and coevaporated with toluene. The residue was dissolved in EtOH (30 mL) and a solution of NaIO<sub>4</sub> (2.37 g, 11.09 mmol) in H<sub>2</sub>O (15 mL) was added dropwise at 0 °C to the reaction mixture. After the mixture was stirred at 0 °C for 20 min, NaBH<sub>4</sub> (1.05 g, 27.76 mmol) was added and the reaction mixture was stirred at 0 °C for 1 h. The reaction mixture was filtered, and the filtrate was evaporated. The residue was purified by silica gel column chromatography (hexanes/EtOAc = 1/1) to give **22** (1.69 g, 85%) as an oil: <sup>1</sup>H NMR (CDCl<sub>3</sub>) δ 5.79 (d, 1 H, *J* = 3.4 Hz), 4.72 (t, 1 H, *J* = 4.1 Hz), 4.09 (m, 1 H), 3.96 (dd, 1 H, *J* = 2.4, 12.5 Hz), 3.66 (dd, 1 H, *J* = 2.9, 12.6 Hz), 3.56 (dd, 1 H, *J* = 4.6, 9.5 Hz), 1.56 (s, 3 H), 1.35 (s, 3 H); IR (KBr): 2108 (N<sub>3</sub>) cm<sup>-1</sup>; FAB-MS *m/z* 216 [M + H]<sup>+</sup>. Anal. (C<sub>8</sub>H<sub>13</sub>N<sub>3</sub>O<sub>4</sub>) C, H, N.

**5-*O*-Acetyl-3-azido-3-deoxy-1,2-*O*-isopropylidene- $\alpha$ -D-ribofuranose (23).** To a stirred solution of **22** (1.5 g, 6.97 mmol) in anhydrous pyridine (15 mL) was added Ac<sub>2</sub>O (1.32 mL, 13.99 mmol). The reaction mixture was stirred at room temperature for 3 h and evaporated. The residue was partitioned between EtOAc and water. The organic layer was washed with brine, dried (MgSO<sub>4</sub>), filtered, and evaporated. The residue was purified by silica gel column chromatography (hexanes/EtOAc = 2/1) to give **23** (1.76 g, 98%) as an oil: <sup>1</sup>H NMR (CDCl<sub>3</sub>) δ 5.78 (d, 1 H, *J* = 3.7 Hz), 4.71 (dd, 1 H, *J* = 3.6, 4.8 Hz), 4.34 (m, 1 H), 4.15–4.26 (m, 2 H), 3.31 (dd, 1 H, *J* = 4.6, 9.5 Hz), 2.08 (s, 3 H), 1.56 (s, 3 H), 1.34 (s, 3 H); IR (KBr): 2109 (N<sub>3</sub>) cm<sup>-1</sup>; FAB-MS *m/z* 258 [M + H]<sup>+</sup>. Anal. (C<sub>10</sub>H<sub>15</sub>N<sub>3</sub>O<sub>5</sub>) C, H, N.

**1,2,5-Tri-*O*-acetyl-3-azido-3-deoxy-D-ribofuranose (24).** A solution of **23** (1.76 g, 6.84 mmol) in 85% formic acid (30 mL) was stirred for 1.5 h at 60 °C and evaporated. The residue was dissolved in pyridine (20 mL) and Ac<sub>2</sub>O (8.39 mL, 88.9 mmol) was added to the reaction mixture. The mixture was stirred at room temperature for 16 h and evaporated. The residue was partitioned between EtOAc and water. The organic layer was washed with brine, dried (MgSO<sub>4</sub>), filtered, and evaporated. The residue was purified by silica gel column chromatography (hexanes/EtOAc = 2/1) to give **24** (2 g, 97%) as an oil: <sup>1</sup>H NMR (CDCl<sub>3</sub>) δ 6.15 (m, 1 H), 5.33 (dd, 1 H, *J* = 4.9, 9.7 Hz), 4.05–4.38 (m, 5 H), 2.09 (m, 9 H); IR (KBr): 2116 (N<sub>3</sub>) cm<sup>-1</sup>; FAB-MS *m/z* 324 [M + Na]<sup>+</sup>. Anal. (C<sub>11</sub>H<sub>15</sub>N<sub>3</sub>O<sub>7</sub>) C, H, N.

**3-Azido-3-deoxy-1,2-*O*-isopropylidene- $\alpha$ -D-ribofuranuronic Acid Methyl Amide (33).** A solution of **21** (2.08 g, 7.29 mmol) in 75% AcOH (30 mL) was stirred at 55 °C for 1.5 h. The reaction mixture was evaporated and the residue was dissolved in CCl<sub>4</sub> (14 mL), CH<sub>3</sub>CN (14 mL), and H<sub>2</sub>O (20 mL). To this solution were added NaIO<sub>4</sub> (6.55 g, 30.6 mmol) and ruthenium trichloride hydrate (33 mg, 0.16 mmol) at room temperature. The reaction mixture was stirred at room temperature for 4 h and filtered through a Celite pad. The filtrate was extracted with CH<sub>2</sub>Cl<sub>2</sub> ( $\times$  3). The combined organic layers were dried (MgSO<sub>4</sub>), filtered, and evaporated to give **32**.

Oxalyl chloride (1.5 mL) was added to a solution of **32** in anhydrous CH<sub>2</sub>Cl<sub>2</sub> (15 mL). DMF (0.5 mL) was added, and the reaction mixture was stirred at room temperature for 16 h and evaporated. The residue was dissolved in anhydrous CH<sub>2</sub>Cl<sub>2</sub> (15 mL) and cooled to 0 °C. A solution of 2 M NH<sub>2</sub>CH<sub>3</sub> in THF (0.37 mL) was added dropwise. After being stirred for 3 h, the mixture was diluted with water and extracted with CH<sub>2</sub>Cl<sub>2</sub> ( $\times$  3). The combined organic layers were dried (MgSO<sub>4</sub>), filtered, and evaporated. The residue was purified by silica gel column chromatography (hexanes/EtOAc = 1/2) to give **33** (772 mg, 44%) as a solid: <sup>1</sup>H NMR (CDCl<sub>3</sub>) δ 6.43 (brs, 1 H), 5.84 (d, 1 H, *J* = 3.3 Hz), 4.71 (dd, 1 H, *J* = 3.3, 4.6 Hz), 4.48 (d, 1 H, *J* = 9.6 Hz), 3.63 (dd, 1 H, *J* = 4.5, 9.5 Hz), 2.86 (d, 1 H, *J* = 5.0 Hz), 1.58 (s, 3 H), 1.38 (s, 3 H); FAB-MS *m/z* 265 [M + Na]<sup>+</sup>. Anal. (C<sub>9</sub>H<sub>14</sub>N<sub>4</sub>O<sub>4</sub>) C, H, N.

**1,2-Di-*O*-acetyl-3-azido-3-deoxy-D-ribofuranuronic Acid Methyl Amide (34).** Compound **33** (772 mg, 3.19 mmol) was dissolved in a solution of AcOH (20 mL) and Ac<sub>2</sub>O (2.4 mL). The mixture was cooled to 0 °C and concd H<sub>2</sub>SO<sub>4</sub> (0.014 mL) was added to this solution. The reaction mixture was stirred at room temperature for 18 h and poured into the saturated NaHCO<sub>3</sub> solution. The mixture was extracted with CH<sub>2</sub>Cl<sub>2</sub> ( $\times$  3). The combined organic layers were washed with brine, dried (MgSO<sub>4</sub>), filtered, and evaporated. The residue was purified by silica gel column chromatography (hexanes/EtOAc = 1/2) to give **34** (750 mg, 82%) as an oil: <sup>1</sup>H NMR (CDCl<sub>3</sub>) δ 6.44 (brs, 1 H), 6.15 (s, 1 H), 5.30 (d, 1 H, *J* = 4.8 Hz), 4.48 (d, 1 H, *J* = 7.2 Hz), 4.39 (dd, 1 H, *J* = 4.8, 7.2 Hz), 2.86 (d, 1 H, *J* = 5.0 Hz), 2.18 (s, 3 H), 2.08 (s, 3 H); IR (KBr): 2120 (N<sub>3</sub>), 1752 (C=O), 1674 (C=O) cm<sup>-1</sup>; FAB-MS *m/z* 287 [M + H]<sup>+</sup>. Anal. (C<sub>10</sub>H<sub>14</sub>N<sub>4</sub>O<sub>6</sub>) C, H, N.

**General Procedure for the Synthesis of 25a, 25b, and 35.** A mixture of 6-chloropurine or 2,6-dichloropurine (2.0 equiv) and ammonium sulfate (catalytic amount) in anhydrous HMDS (30 mL) was refluxed under nitrogen atmosphere for 16 h and concentrated under anhydrous conditions. The residue was dissolved in anhydrous 1,2-dichloroethane (20 mL), and a solution of **24** and **34** in 1,2-dichloroethane (20 mL) was added to this solution followed by addition of TMSOTf (2.0 equiv) at 0 °C. The reaction mixture was stirred at room temperature for 20 min and then at 60 °C for 2 h. The mixture was quenched by addition of saturated NaHCO<sub>3</sub> solution and filtered through a Celite pad. The filtrate was extracted with CH<sub>2</sub>Cl<sub>2</sub> ( $\times$  3). The combined organic layers were dried (MgSO<sub>4</sub>), filtered, and evaporated. The residue was purified by silica gel column chromatography to give **25a**, **25b**, and **35**.

**9-(2,3-Di-*O*-acetyl-3-azido-3-deoxy- $\beta$ -D-ribofuranosyl)-6-chloropurine (25a).** 67% yield; white foam; <sup>1</sup>H NMR (CDCl<sub>3</sub>) δ 8.78 (s, 1 H), 8.25 (s, 1 H), 6.12 (d, 1 H, *J* = 3.5 Hz), 5.98 (dd, 1 H, *J* = 5.9, 3.5 Hz), 4.71 (t, 1 H, *J* = 6.3), 4.29–4.40 (m, 3 H), 2.21 (s,

3 H), 2.09 (s, 3 H); IR (KBr): 2115 (N<sub>3</sub>), 1746 (C=O) cm<sup>-1</sup>; FAB-MS *m/z* 396 [M + H]<sup>+</sup>. Anal. (C<sub>14</sub>H<sub>14</sub>ClN<sub>7</sub>O<sub>5</sub>) C, H, N.

**9-(2,3-Di-*O*-acetyl-3-azido-3-deoxy-β-D-ribofuranosyl)-2,6-dichloropurine (25b).** 51% yield; white foam; <sup>1</sup>H NMR (CDCl<sub>3</sub>) δ 8.24 (s, 1 H), 6.10 (d, 1 H, *J* = 3.9 Hz), 5.84 (dd, 1 H, *J* = 3.9, 5.7 Hz), 4.61 (m, 1 H), 4.29–4.50 (m, 3 H), 2.22 (s, 3 H), 2.12 (s, 3 H); IR (KBr): 2116 (N<sub>3</sub>), 1745 (C=O) cm<sup>-1</sup>; FAB-MS *m/z* 431 [M + H]<sup>+</sup>. Anal. (C<sub>14</sub>H<sub>13</sub>Cl<sub>2</sub>N<sub>7</sub>O<sub>5</sub>) C, H, N.

**3-Azido-5-(6-chloro-purin-9-yl)-4-acetoxy-tetrahydro-furan-2-carboxylic Acid Methyl Amide (35).** 73% yield; white foam; <sup>1</sup>H NMR (CDCl<sub>3</sub>) δ 8.78 (s, 1 H), 8.25 (s, 1 H), 7.62 (brs, 1 H), 6.15 (d, 1 H, *J* = 7.0 Hz), 5.87 (dd, 1 H, *J* = 5.7, 7.0 Hz), 4.86 (dd, 1 H, *J* = 3.1, 5.7 Hz), 4.58 (d, 1 H, *J* = 3.1 Hz), 2.92 (d, 1 H, *J* = 5.0 Hz), 2.05 (s, 3 H); IR (KBr): 2117 (N<sub>3</sub>), 1751 (C=O), 1673 (C=O) cm<sup>-1</sup>; FAB-MS *m/z* 381 [M + H]<sup>+</sup>. Anal. (C<sub>13</sub>H<sub>13</sub>-ClN<sub>8</sub>O<sub>4</sub>) C, H, N.

**General Procedure for the Synthesis of 26a and 36.** A mixture of **25a** and **35** and 40% methylamine in water (4 mL) in 1,4-dioxane (10 mL) was stirred at room temperature for 4 h. The reaction mixture was evaporated, and the residue was purified by silica gel column chromatography to give **26a** and **36**, respectively.

**N<sup>6</sup>-Methyl-9-(3-azido-3-deoxy-β-D-ribofuranosyl)adenine (26a).** 90% yield; white solid; <sup>1</sup>H NMR (DMSO-*d*<sub>6</sub>) δ 8.31 (s, 1 H), 8.20 (s, 1 H), 7.83 (brs, 1 H), 6.18 (d, 1 H, *J* = 5.7 Hz), 5.86 (d, 1 H, *J* = 6.1 Hz), 5.56 (dd, 1 H, *J* = 4.5, 7.6 Hz), 4.95 (dd, 1 H, *J* = 5.7, 11.4 Hz), 4.27 (dd, 1 H, *J* = 3.5, 5.4 Hz), 3.93 (dd, 1 H, *J* = 3.3, 6.8 Hz), 3.50–3.69 (m, 2 H), 2.92 (s, 3 H); IR (KBr): 3430 (OH), 2104 (N<sub>3</sub>), 1634 (C=O) cm<sup>-1</sup>; FAB-MS *m/z* 307 [M + H]<sup>+</sup>. Anal. (C<sub>11</sub>H<sub>14</sub>N<sub>8</sub>O<sub>3</sub>) C, H, N.

**3-Azido-5-(6-methylaminopurin-9-yl)-4-hydroxy-tetrahydro-furan-2-carboxylic Acid Methyl Amide (36).** 87% yield; white solid; <sup>1</sup>H NMR (DMSO-*d*<sub>6</sub>) δ 8.69 (d, 1 H, *J* = 4.4 Hz), 8.38 (s, 1 H), 8.27 (s, 1 H), 7.87 (brs, 1 H), 6.58 (d, 1 H, *J* = 5.5 Hz), 5.95 (d, 1 H, *J* = 6.4 Hz), 4.90 (dd, 1 H, *J* = 5.6, 11.4 Hz), 4.45 (dd, 1 H, *J* = 3.0, 5.0 Hz), 4.29 (d, 1 H, *J* = 2.9 Hz), 2.93 (s, 3 H), 2.66 (d, 3 H, *J* = 4.6 Hz); IR (KBr): 3379 (OH), 2123 (N<sub>3</sub>), 1662 (C=O) cm<sup>-1</sup>; FAB-MS *m/z* 334 [M + H]<sup>+</sup>. Anal. (C<sub>12</sub>H<sub>15</sub>N<sub>9</sub>O<sub>3</sub>) C, H, N.

**General Procedure for the Synthesis of 26b, 26c, and 15.** A mixture of **25a**, **25b**, **15**, 3-iodobenzylamine hydrochloride (1.1 equiv), and Et<sub>3</sub>N (3.0 equiv) in EtOH (10 mL) was stirred at 50 °C for 18 h. The reaction mixture was evaporated, and the residue was partitioned between CH<sub>2</sub>Cl<sub>2</sub> and water. The organic layer was washed with brine, dried (MgSO<sub>4</sub>), filtered, and evaporated. The residue was dissolved in MeOH (10 mL), and 28% NaOMe (1 mL) was added to this solution. The reaction mixture was stirred at room temperature for 2 h and evaporated. The residue was purified by silica gel column chromatography to give **26b**, **26c**, and **15**, respectively.

**N<sup>6</sup>-(3-Iodobenzyl)-9-(3-azido-3-deoxy-β-D-ribofuranosyl)adenine (26b).** 86% yield; solid; <sup>1</sup>H NMR (DMSO-*d*<sub>6</sub>) δ 8.60 (s, 1 H), 8.47 (s, 1 H), 8.29 (s, 1 H), 7.78 (s, 1 H), 7.63 (d, 1 H, *J* = 7.9 Hz), 7.40 (d, 1 H, *J* = 7.4 Hz), 7.14 (t, 1 H, *J* = 7.9 Hz), 6.28 (d, 1 H, *J* = 5.3 Hz), 5.97 (d, 1 H, *J* = 5.8 Hz), 5.57 (dd, 1 H, *J* = 4.6, 7.1 Hz), 5.05 (m, 1 H), 4.73 (m, 2 H), 4.37 (m, 1 H), 4.05 (m, 1 H), 3.72 (m, 1 H), 3.62 (m, 1 H); IR (KBr): 3426 (OH), 2106 (N<sub>3</sub>), 1622 (C=O) cm<sup>-1</sup>; FAB-MS *m/z* 590 [M + H]<sup>+</sup>. Anal. (C<sub>17</sub>H<sub>17</sub>IN<sub>8</sub>O<sub>3</sub>) C, H, N.

**2-Chloro-N<sup>6</sup>-(3-iodobenzyl)-9-(3-azido-3-deoxy-β-D-ribofuranosyl)adenine (26c).** 95% yield; solid; <sup>1</sup>H NMR (DMSO-*d*<sub>6</sub>) δ 7.71 (s, 1 H), 7.69 (s, 1 H), 7.59 (d, 1 H, *J* = 7.9 Hz), 7.26 (m, 1 H), 7.02 (t, 1 H, *J* = 7.7 Hz), 6.55 (s, 1 H), 5.97 (d, 1 H, *J* = 10.1 Hz), 5.70 (d, 1 H, *J* = 7.3 Hz), 5.24 (m, 1 H), 4.64–4.77 (m, 3 H), 4.31 (d, 1 H, *J* = 5.1 Hz), 4.19 (s, 1 H), 3.94 (d, 1 H, *J* = 12.81 Hz), 3.68 (m, 1 H); IR (KBr): 3305 (OH), 2112 (N<sub>3</sub>), 1621 (C=O) cm<sup>-1</sup>; FAB-MS *m/z* 543 [M + H]<sup>+</sup>. Anal. (C<sub>17</sub>H<sub>16</sub>ClIN<sub>8</sub>O<sub>3</sub>) C, H, N.

**3-Azido-5-(6-(3-iodobenzylamino)purin-9-yl)-4-hydroxy-tetrahydro-furan-2-carboxylic Acid Methyl Amide (15).** 89% yield; white solid; <sup>1</sup>H NMR (CDCl<sub>3</sub>) δ 8.61 (d, 1 H, *J* = 4.4 Hz), 8.28 (s, 1 H), 7.71 (s, 1 H), 7.69 (s, 1 H), 7.60 (d, 1 H, *J* = 7.8 Hz), 7.30

(d, 1 H, *J* = 7.7 Hz), 7.04 (t, 1 H, *J* = 7.7 Hz), 6.48 (brs, 1 H), 5.79 (d, 1 H, *J* = 7.1 Hz), 5.07 (m, 2 H), 4.77 (m, 2 H), 4.48 (m, 2 H), 2.85 (d, 1 H, *J* = 4.9 Hz); FAB-MS *m/z* 536 [M + H]<sup>+</sup>. Anal. (C<sub>18</sub>H<sub>18</sub>IN<sub>9</sub>O<sub>3</sub>) C, H, N.

**General Procedure for the Synthesis of 27a–c and 37a,b.** A mixture of **26a–c**, **36**, **15**, imidazole (5 equiv), and TBSCl (2.5 equiv) in anhydrous DMF (15 mL) was stirred at room temperature for 24 h. The reaction mixture was poured into water (200 mL) and extracted with ethyl acetate (× 3). The combined organic layers were dried (MgSO<sub>4</sub>), filtered, and evaporated. The residue was purified by silica gel column chromatography to give **27a–c** and **37a,b**, respectively.

**N<sup>6</sup>-Methyl-9-(3-azido-2,5-di-*O*-*t*-butyldimethylsilyl-3-deoxy-β-D-ribofuranosyl)adenine (27a).** 76% yield; oil; <sup>1</sup>H NMR (CDCl<sub>3</sub>) δ 8.24 (s, 1 H), 7.94 (s, 1 H), 5.87 (d, 1 H, *J* = 4.0 Hz), 5.72 (brs, 1 H), 4.73 (dd, 1 H, *J* = 4.0, 5.0 Hz), 4.06 (m, 1 H), 3.91–3.97 (m, 2 H), 3.67 (dd, 1 H, *J* = 2.8, 11.6 Hz), 3.05 (d, 3 H, *J* = 4.6 Hz), 0.82 (s, 9 H), 0.73 (s, 9 H), 0.11 (s, 3 H), 0.00 (s, 3 H), -0.08 (s, 3 H), -0.19 (s, 3 H); IR (KBr): 2107 (N<sub>3</sub>) cm<sup>-1</sup>; FAB-MS *m/z* 535 [M + H]<sup>+</sup>. Anal. (C<sub>23</sub>H<sub>42</sub>N<sub>8</sub>O<sub>3</sub>Si<sub>2</sub>) C, H, N.

**N<sup>6</sup>-(3-Iodobenzyl)-9-(3-azido-2,5-di-*O*-*t*-butyldimethylsilyl-3-deoxy-β-D-ribofuranosyl)adenine (27b).** 84% yield; oil; <sup>1</sup>H NMR (CDCl<sub>3</sub>) δ 8.24 (s, 1 H), 7.98 (s, 1 H), 7.59 (s, 1 H), 7.46 (d, 1 H, *J* = 7.8 Hz), 7.19 (d, 1 H, *J* = 7.7 Hz), 6.90 (t, 1 H, *J* = 7.7 Hz), 5.99 (brs, 1 H), 5.88 (d, 1 H, *J* = 3.9 Hz), 4.70–4.75 (m, 3 H), 4.07 (m, 1 H), 3.91–3.97 (m, 2 H), 3.68 (dd, 1 H, *J* = 2.6, 11.6 Hz), 0.81 (s, 9 H), 0.74 (s, 9 H), 0.01 (s, 3 H), 0.00 (s, 3 H), -0.06 (s, 3 H), -0.16 (s, 3 H); IR (KBr): 2106 (N<sub>3</sub>) cm<sup>-1</sup>; FAB-MS *m/z* 737 [M + H]<sup>+</sup>. Anal. (C<sub>29</sub>H<sub>45</sub>IN<sub>8</sub>O<sub>3</sub>Si<sub>2</sub>) C, H, N.

**2-Chloro-N<sup>6</sup>-(3-iodobenzyl)-9-(3-azido-2,5-di-*O*-*t*-butyldimethylsilyl-3-deoxy-β-D-ribofuranosyl)adenine (27c).** 83% yield; oil; <sup>1</sup>H NMR (CDCl<sub>3</sub>) δ 8.24 (s, 1 H), 7.99 (s, 1 H), 7.57 (s, 1 H), 7.47 (d, 1 H, *J* = 7.9 Hz), 7.18 (d, 1 H, *J* = 7.7 Hz), 6.90 (t, 1 H, *J* = 7.9 Hz), 6.05 (brs, 1 H), 5.82 (d, 1 H, *J* = 3.3 Hz), 4.62 (m, 3 H), 4.08 (m, 1 H), 3.93 (dd, 1 H, *J* = 2.9, 11.7 Hz), 3.82 (dd, 1 H, *J* = 4.8, 6.2 Hz), 3.67 (dd, 1 H, *J* = 2.4, 11.6 Hz), 0.80 (s, 9 H), 0.76 (s, 9 H), 0.02 (s, 3 H), 0.00 (s, 3 H), -0.03 (s, 3 H), -0.10 (s, 3 H); IR (KBr): 2106 (N<sub>3</sub>) cm<sup>-1</sup>; FAB-MS *m/z* 771 [M]<sup>+</sup>. Anal. (C<sub>29</sub>H<sub>44</sub>ClIN<sub>8</sub>O<sub>3</sub>Si<sub>2</sub>) C, H, N.

**3-Azido-5-(6-methylaminopurin-9-yl)-4-*t*-butyldimethylsilyloxy-tetrahydro-furan-2-carboxylic Acid Methyl Amide (37a).** 83% yield; foam; <sup>1</sup>H NMR (CDCl<sub>3</sub>) δ 9.31 (brs, 1 H), 8.49 (s, 1 H), 7.88 (s, 1 H), 6.10 (d, 1 H, *J* = 4.6 Hz), 5.89 (d, 1 H, *J* = 8.1 Hz), 5.19 (dd, 1 H, *J* = 5.1, 8.1 Hz), 4.59 (s, 1 H), 4.40 (d, 1 H, *J* = 5.1 Hz), 3.33 (brs, 3 H), 3.06 (d, 1 H, *J* = 4.8 Hz), 0.87 (s, 9 H), 0.00 (s, 3 H), -0.36 (s, 3 H); IR (KBr): 2105 (N<sub>3</sub>) cm<sup>-1</sup>; FAB-MS *m/z* 448 [M + H]<sup>+</sup>. Anal. (C<sub>18</sub>H<sub>29</sub>N<sub>9</sub>O<sub>3</sub>Si) C, H, N.

**3-Azido-5-(6-(3-iodobenzylamino)purin-9-yl)-4-*t*-butyldimethylsilyloxy-tetrahydro-furan-2-carboxylic Acid Methyl Amide (37b).** 71% yield; foam; <sup>1</sup>H NMR (CDCl<sub>3</sub>) δ 9.22 (d, 1 H, *J* = 4.2 Hz), 8.48 (s, 1 H), 7.88 (s, 1 H), 7.82 (s, 1 H), 7.72 (d, 1 H, *J* = 7.9 Hz), 7.43 (d, 1 H, *J* = 7.7 Hz), 7.16 (t, 1 H, *J* = 7.7 Hz), 6.37 (t, 1 H, *J* = 6.0 Hz), 5.88 (d, 1 H, *J* = 7.9 Hz), 5.18 (dd, 1 H, *J* = 5.2, 7.9 Hz), 4.90 (brs, 2 H), 4.59 (s, 1 H), 4.40 (d, 1 H, *J* = 5.1 Hz), 3.05 (d, 1 H, *J* = 5.8 Hz), 0.87 (s, 9 H), 0.00 (3, 3 H), -0.36 (s, 3 H); IR (KBr): 2105 (N<sub>3</sub>) cm<sup>-1</sup>; FAB-MS *m/z* 672 [M + Na]<sup>+</sup>. Anal. (C<sub>24</sub>H<sub>32</sub>IN<sub>9</sub>O<sub>3</sub>Si) C, H, N.

**General Procedure for the Synthesis of 28a–c and 38a,b.** To a stirred solution of **27a–c** and **37a,b** in THF (15 mL) was added triphenylphosphine (1.5 equiv) at 0 °C. After being stirred for 30 min, NH<sub>4</sub>OH (1.8 mL) and H<sub>2</sub>O (0.3 mL) were added to the reaction mixture. The mixture was stirred overnight at room temperature and evaporated. The residue was purified by silica gel column chromatography to give **28a–c** and **38a,b**, respectively.

**N<sup>6</sup>-Methyl-9-(3-amino-2,5-di-*O*-*t*-butyldimethylsilyl-3-deoxy-β-D-ribofuranosyl)adenine (28a).** 88% yield; foam; <sup>1</sup>H NMR (CDCl<sub>3</sub>) δ 8.24 (s, 1 H), 8.13 (s, 1 H), 5.89 (d, 1 H, *J* = 1.7 Hz), 5.75 (dd, 1 H, *J* = 5.9, 3.5 Hz), 4.24 (dd, 1 H, *J* = 1.7, 4.8 Hz), 3.93 (m, 1 H), 3.74–3.82 (m, 2 H), 3.45 (dd, 1 H, *J* = 4.8, 8.3 Hz), 3.03 (d, 3 H, *J* = 5.0 Hz), 0.81 (s, 9 H), 0.80 (s, 9 H), 0.07

(s, 3 H), 0.01 (s, 3 H), 0.00 (s, 3 H), -0.02 (s, 3 H); IR (KBr): 3290, 2931, 1624, 1119, 838 cm<sup>-1</sup>; FAB-MS *m/z* 509 [M + H]<sup>+</sup>. Anal. (C<sub>23</sub>H<sub>44</sub>N<sub>6</sub>O<sub>3</sub>Si<sub>2</sub>) C, H, N.

**N<sup>6</sup>-(3-Iodobenzyl)-9-(3-amino-2,5-di-*O*-*t*-butyldimethylsilyl-3-deoxy-β-D-ribofuranosyl)adenine (28b).** 96% yield; foam; <sup>1</sup>H NMR (CDCl<sub>3</sub>) δ 8.24 (s, 1 H), 8.17 (s, 1 H), 7.60 (s, 1 H), 7.45 (d, 1 H, *J* = 7.0 Hz), 7.20 (d, 1 H, *J* = 7.7 Hz), 6.90 (t, 1 H, *J* = 7.7 Hz), 6.00 (brs, 1 H), 5.90 (d, 1 H, *J* = 1.7 Hz), 4.68 (brs, 2 H), 4.23 (dd, 1 H, *J* = 1.5, 4.6 Hz), 3.94 (m, 1 H), 3.74–3.82 (m, 2 H), 3.45 (dd, 1 H, *J* = 4.7, 8.4 Hz), 0.81 (s, 9 H), 0.80 (s, 9 H), 0.08 (s, 3 H), 0.02 (s, 3 H), 0.01 (s, 3 H), 0.00 (s, 3 H); IR (KBr): 2931, 1618, 1469, 1120, 839, 780 cm<sup>-1</sup>; FAB-MS *m/z* 711 [M + H]<sup>+</sup>. Anal. (C<sub>29</sub>H<sub>47</sub>N<sub>6</sub>O<sub>3</sub>Si<sub>2</sub>) C, H, N.

**2-Chloro-N<sup>6</sup>-(3-iodobenzyl)-9-(3-amino-2,5-di-*O*-*t*-butyldimethylsilyl-3-deoxy-β-D-ribofuranosyl)adenine (28c).** 94% yield; foam; <sup>1</sup>H NMR (CDCl<sub>3</sub>) δ 8.18 (s, 1 H), 7.59 (s, 1 H), 7.47 (d, 1 H, *J* = 7.9 Hz), 7.19 (d, 1 H, *J* = 7.7 Hz), 6.91 (t, 1 H, *J* = 7.7 Hz), 6.08 (brs, 1 H), 5.82 (d, 1 H, *J* = 1.1 Hz), 4.63 (s, 2 H), 4.17 (d, 1 H, *J* = 4.7 Hz), 3.96 (dd, 1 H, *J* = 2.4, 11.5 Hz), 3.74–3.80 (m, 2 H), 3.38 (dd, 1 H, *J* = 4.4, 8.8 Hz), 0.82 (s, 9 H), 0.81 (s, 9 H), 0.15 (s, 3 H), 0.03 (s, 3 H), 0.02 (s, 3 H), 0.00 (s, 3 H); IR (KBr): 2930, 1618, 1466, 1314, 1121, 838, 780 cm<sup>-1</sup>; FAB-MS *m/z* 746 [M + H]<sup>+</sup>. Anal. (C<sub>29</sub>H<sub>46</sub>ClIN<sub>6</sub>O<sub>3</sub>Si<sub>2</sub>) C, H, N.

**3-Amino-5-(6-methylaminopurin-9-yl)-4-*t*-butyldimethylsilyloxy-tetrahydro-furan-2-carboxylic Acid Methyl Amide (38a).** 95% yield; oil; <sup>1</sup>H NMR (CD<sub>3</sub>OD) δ 8.37 (s, 1 H), 8.35 (s, 1 H), 6.09 (d, 1 H, *J* = 5.5 Hz), 4.85 (dd, 1 H, *J* = 5.5, 11.0 Hz), 4.39 (d, 1 H, *J* = 3.8 Hz), 3.72 (m, 1 H), 3.15 (brs, 3 H), 2.90 (s, 3 H), 0.87 (s, 9 H), 0.00 (s, 3 H), -0.16 (s, 3 H); IR (KBr): 3431, 2930, 1629, 1054, 833, 643 cm<sup>-1</sup>; FAB-MS *m/z* 422 [M + H]<sup>+</sup>. Anal. (C<sub>18</sub>H<sub>31</sub>N<sub>7</sub>O<sub>3</sub>Si) C, H, N.

**3-Amino-5-(6-(3-iodobenzylamino)purin-9-yl)-4-*t*-butyldimethylsilyloxy-tetrahydro-furan-2-carboxylic Acid Methyl Amide (38b).** 94% yield; oil; <sup>1</sup>H NMR (CDCl<sub>3</sub>) δ 8.99 (brs, 1 H), 8.50 (s, 1 H), 7.91 (s, 1 H), 7.85 (s, 1 H), 7.74 (d, 1 H, *J* = 7.8 Hz), 7.45 (d, 1 H, *J* = 7.7 Hz), 7.17 (t, 1 H, *J* = 7.9 Hz), 6.35 (brs, 1 H), 6.11 (d, 1 H, *J* = 6.6 Hz), 4.91 (m, 3 H), 4.56 (s, 1 H), 3.93 (dd, 1 H, *J* = 2.6, 5.5 Hz), 3.05 (d, 1 H, *J* = 4.7 Hz), 0.92 (s, 9 H), 0.00 (s, 3 H), -0.21 (s, 3 H); IR (KBr): 3272, 2931, 1670, 1619, 1473, 1338, 1253, 1151, 1059, 839, 754 cm<sup>-1</sup>; FAB-MS *m/z* 624 [M + H]<sup>+</sup>. Anal. (C<sub>24</sub>H<sub>34</sub>IN<sub>7</sub>O<sub>3</sub>Si) C, H, N.

**General Procedure for the Synthesis of 29a–c and 39a,b.** To a stirred solution of 28a–c and 38a,b in anhydrous DMF (10 mL) was added chloroacetyl isocyanate (1.1 equiv) at 0 °C. After being stirred for 2 h at 0 °C, the reaction mixture was evaporated and the residue was purified by silica gel column chromatography to give 29a–c and 38a,b.

**N<sup>6</sup>-Methyl-9-(3-chloroacetylureido-2,5-di-*O*-*t*-butyldimethylsilyl-3-deoxy-β-D-ribofuranosyl)adenine (29a).** 87% yield; oil; <sup>1</sup>H NMR (CDCl<sub>3</sub>) δ 8.41 (m, 2 H), 8.25 (s, 1 H), 8.10 (s, 1 H), 5.94 (d, 1 H, *J* = 2.6 Hz), 5.72 (brs, 1 H), 4.47–4.55 (m, 2 H), 4.12 (m, 1 H), 3.99 (s, 2 H), 3.90 (dd, 1 H, *J* = 2.0, 11.5 Hz), 3.72 (dd, 1 H, *J* = 3.0, 11.5 Hz), 3.06 (d, 3 H, *J* = 4.7 Hz), 0.81 (s, 9 H), 0.75 (s, 9 H), 0.00 (s, 6 H), -0.07 (s, 3 H), -0.12 (s, 3 H); IR (KBr): 3303, 2953, 1702, 1623, 1536, 1254, 1229, 1127, 837 cm<sup>-1</sup>; FAB-MS *m/z* 629 [M + H]<sup>+</sup>.

**N<sup>6</sup>-(3-Iodobenzyl)-9-(3-chloroacetylureido-2,5-di-*O*-*t*-butyldimethylsilyl-3-deoxy-β-D-ribofuranosyl)adenine (29b).** 77% yield; foam; <sup>1</sup>H NMR (CDCl<sub>3</sub>) δ 8.39 (m, 2 H), 8.25 (s, 1 H), 8.15 (s, 1 H), 7.60 (s, 1 H), 7.46 (d, 1 H, *J* = 8.0 Hz), 7.20 (d, 1 H, *J* = 7.7 Hz), 6.90 (t, 1 H, *J* = 7.9 Hz), 6.02 (brs, 1 H), 5.95 (d, 1 H, *J* = 2.2 Hz), 4.69 (brs, 2 H), 4.48–4.55 (m, 2 H), 4.12 (m, 1 H), 3.99 (s, 2 H), 3.91 (dd, 1 H, *J* = 2.2, 11.7 Hz), 3.72 (dd, 1 H, *J* = 2.7, 11.7 Hz), 0.82 (s, 9 H), 0.75 (s, 9 H), 0.00 (s, 6 H), -0.04 (s, 3 H), -0.10 (s, 3 H); IR (KBr): 3299, 2932, 1701, 1617, 1473, 1254, 1126, 838, 781 cm<sup>-1</sup>; FAB-MS *m/z* 831 [M + H]<sup>+</sup>.

**2-Chloro-N<sup>6</sup>-(3-iodobenzyl)-9-(3-chloroacetylureido-2,5-di-*O*-*t*-butyldimethylsilyl-3-deoxy-β-D-ribofuranosyl)adenine (29c).** 81% yield; foam; <sup>1</sup>H NMR (CDCl<sub>3</sub>) δ 8.38 (s, 1 H), 8.31 (s, 1 H), 8.19 (s, 1 H), 7.59 (s, 1 H), 7.47 (d, 1 H, *J* = 7.7 Hz), 7.19 (d,

1 H, *J* = 7.9 Hz), 6.91 (t, 1 H, *J* = 7.9 Hz), 6.08 (brs, 1 H), 5.88 (d, 1 H, *J* = 1.8 Hz), 4.63 (s, 2 H), 4.42–4.51 (m, 2 H), 4.11 (m, 1 H), 3.99 (s, 2 H), 3.93 (dd, 1 H, *J* = 2.2, 11.9 Hz), 3.69 (dd, 1 H, *J* = 2.4, 11.7 Hz), 0.81 (s, 9 H), 0.78 (s, 9 H), 0.04 (s, 3 H) 0.00 (s, 6 H), -0.04 (s, 3 H); IR (KBr): 3296, 2952, 1700, 1618, 1537, 1470, 1314, 1223, 1127, 837, 781 cm<sup>-1</sup>; FAB-MS *m/z* 863 [M + H]<sup>+</sup>.

**3-Chloroacetylureido-5-(6-methylaminopurin-9-yl)-4-*t*-butyldimethylsilyloxy-tetrahydro-furan-2-carboxylic Acid Methyl Amide (39a).** 94% yield; oil; <sup>1</sup>H NMR (CDCl<sub>3</sub>) δ 8.92 (d, 1 H, *J* = 5.1 Hz), 8.53 (d, 1 H, *J* = 4.6 Hz), 8.47 (s, 1 H), 7.96 (s, 1 H), 6.71 (brs, 1 H), 6.51 (brs, 1 H), 6.26 (d, 1 H, *J* = 4.2 Hz), 5.96 (d, 1 H, *J* = 5.7 Hz), 5.01 (t, 1 H, *J* = 7.9 Hz), 4.74–4.81 (m, 2 H), 4.13 (s, 2 H), 3.29 (brs, 3 H), 2.98 (d, 1 H, *J* = 4.7 Hz), 0.86 (s, 9 H), 0.00 (s, 3 H), -0.20 (s, 3 H); IR (KBr): 3296, 2953, 1703, 1626, 1536, 1237, 1155, 840, 756 cm<sup>-1</sup>; FAB-MS *m/z* 542 [M + H]<sup>+</sup>.

**3-Chloroacetylureido-5-(6-(3-iodobenzylamino)purin-9-yl)-4-*t*-butyldimethylsilyloxy-tetrahydro-furan-2-carboxylic Acid Methyl Amide (39b).** 88% yield; oil; <sup>1</sup>H NMR (CDCl<sub>3</sub>) δ 8.87 (s, 1 H), 8.46 (s, 1 H), 8.31 (s, 1 H), 7.97 (s, 1 H), 7.80 (s, 1 H), 7.63 (d, 1 H, *J* = 7.8 Hz), 7.39 (d, 1 H, *J* = 7.7 Hz), 7.11 (t, 1 H, *J* = 7.7 Hz), 6.42 (m, 2 H), 6.00 (s, 1 H), 5.96 (d, 1 H, *J* = 5.5 Hz), 4.76–5.00 (m, 5 H), 4.22 (s, 2 H), 2.97 (d, 3 H, *J* = 4.8 Hz), 0.85 (s, 9 H), 0.00 (s, 3 H), -0.18 (s, 3 H); IR (KBr): 3290, 2952, 1705, 1619, 1535, 1225, 841, 755 cm<sup>-1</sup>; FAB-MS *m/z* 744 [M + H]<sup>+</sup>.

**General Procedure for the Synthesis of 30a–c and 40a,b.** To a stirred solution of 29a–c and 39a,b in MeOH (10 mL) was added 28% NaOMe (0.27 mL) at room temperature. The reaction mixture was stirred for 18 h at room temperature and evaporated. The residue was purified by silica gel column chromatography to give 30a–c and 40a,b.

**N<sup>6</sup>-Methyl-9-(2,5-di-*O*-*t*-butyldimethylsilyl-3-deoxy-3-ureido-β-D-ribofuranosyl)adenine (30a).** 75% yield; foam; <sup>1</sup>H NMR (CDCl<sub>3</sub>) δ 8.25 (s, 1 H), 8.01 (s, 1 H), 5.90 (d, 1 H, *J* = 3.5 Hz), 5.79 (brs, 1 H), 4.96 (d, 1 H, *J* = 6.1 Hz), 4.66 (s, 2 H), 4.55 (m, 1 H), 4.24 (dd, 1 H, *J* = 6.1, 12.3 Hz), 4.05 (m, 1 H), 3.89 (dd, 1 H, *J* = 2.2, 11.5 Hz), 3.76 (dd, 1 H, *J* = 2.6, 11.7 Hz), 3.08 (d, 3 H, *J* = 4.4 Hz), 0.81 (s, 9 H), 0.75 (s, 9 H), 0.00 (s, 3 H), -0.01 (s, 3 H), -0.10 (s, 3 H), -0.11 (s, 3 H); IR (KBr): 3328, 2932, 1624, 1256, 1125, 837, 782 cm<sup>-1</sup>; FAB-MS *m/z* 552 [M + H]<sup>+</sup>. Anal. (C<sub>24</sub>H<sub>45</sub>N<sub>7</sub>O<sub>4</sub>Si<sub>2</sub>) C, H, N.

**N<sup>6</sup>-(3-Iodobenzyl)-9-(2,5-di-*O*-*t*-butyldimethylsilyl-3-deoxy-3-ureido-β-D-ribofuranosyl)adenine (30b).** 89% yield; foam; <sup>1</sup>H NMR (CDCl<sub>3</sub>) δ 8.25 (s, 1 H), 8.05 (s, 1 H), 7.61 (s, 1 H), 7.48 (d, 1 H, *J* = 7.7 Hz), 7.21 (d, 1 H, *J* = 7.7 Hz), 6.92 (t, 1 H, *J* = 7.7 Hz), 6.00 (brs, 1 H), 5.90 (d, 1 H, *J* = 3.1 Hz), 4.86 (d, 1 H, *J* = 6.9 Hz), 4.72 (brs, 2 H), 4.57 (m, 3 H), 4.25 (dd, 1 H, *J* = 6.8, 12.4 Hz), 4.04 (m, 1 H), 3.90 (dd, 1 H, *J* = 2.2, 11.7 Hz), 3.75 (dd, 1 H, *J* = 2.4, 11.5 Hz), 0.81 (s, 9 H), 0.76 (s, 9 H), 0.00 (s, 3 H), -0.01 (s, 3 H), -0.05 (s, 3 H), -0.08 (s, 3 H); IR (KBr): 3306, 2931, 1671, 1617, 1471, 1336, 1256, 1125, 837, 781 cm<sup>-1</sup>; FAB-MS *m/z* 754 [M + H]<sup>+</sup>. Anal. (C<sub>30</sub>H<sub>48</sub>IN<sub>7</sub>O<sub>4</sub>Si<sub>2</sub>) C, H, N.

**2-Chloro-N<sup>6</sup>-(3-iodobenzyl)-9-(2,5-di-*O*-*t*-butyldimethylsilyl-3-deoxy-3-urido-β-D-ribofuranosyl)adenine (30c).** 91% yield; foam; <sup>1</sup>H NMR (CDCl<sub>3</sub>) δ 8.06 (s, 1 H), 7.60 (s, 1 H), 7.49 (d, 1 H, *J* = 7.9 Hz), 7.20 (d, 1 H, *J* = 7.7 Hz), 6.92 (t, 1 H, *J* = 7.7 Hz), 6.19 (brs, 1 H), 5.85 (d, 1 H, *J* = 3.1 Hz), 4.89 (d, 1 H, *J* = 6.9 Hz), 4.66 (s, 4 H), 4.46 (m, 1 H), 4.21 (dd, 1 H, *J* = 6.8, 12.5 Hz), 4.04 (m, 1 H), 3.90 (dd, 1 H, *J* = 2.2, 11.7 Hz), 3.73 (dd, 1 H, *J* = 2.2, 11.7 Hz), 0.80 (s, 9 H), 0.77 (s, 9 H), 0.00 (s, 6 H), -0.02 (s, 3 H), -0.05 (s, 3 H); IR (KBr): 3307, 2931, 1671, 1617, 1468, 1311, 1256, 1125, 837, 781 cm<sup>-1</sup>; FAB-MS *m/z* 788 [M + H]<sup>+</sup>. Anal. (C<sub>30</sub>H<sub>47</sub>ClIN<sub>7</sub>O<sub>4</sub>Si<sub>2</sub>) C, H, N.

**3-Ureido-5-(6-methylaminopurin-9-yl)-4-*t*-butyldimethylsilyloxy-tetrahydro-furan-2-carboxylic Acid Methyl Amide (40a).** 72% yield; oil; <sup>1</sup>H NMR (CDCl<sub>3</sub>) δ 8.69 (brs, 1 H), 8.37 (s, 1 H), 7.79 (s, 1 H), 5.95 (brs, 1 H), 5.78 (d, 1 H, *J* = 7.2 Hz), 5.37 (brs, 1 H), 4.95 (t, 1 H, *J* = 7.4 Hz), 4.74 (d, 1 H, *J* = 2.1 Hz), 4.05 (m, 1 H), 3.23 (brs, 3 H), 2.95 (d, 1 H, *J* = 5.0 Hz), 0.78 (s, 9 H), -0.13 (s,

3 H), -0.32 (s, 3 H); IR (KBr): 3301, 2933, 1668, 1625, 1377, 1252, 1116, 840, 755 cm<sup>-1</sup>; FAB-MS *m/z* 465 [M + H]<sup>+</sup>. Anal. (C<sub>19</sub>H<sub>32</sub>N<sub>8</sub>O<sub>4</sub>Si) C, H, N.

**3-Ureido-5-(6-(3-iodobenzylamino)purin-9-yl)-4-*t*-butyldimethylsilyloxy-tetrahydro-furan-2-carboxylic Acid Methyl Amide (40b).** 72% yield; oil; <sup>1</sup>H NMR (CDCl<sub>3</sub>) δ 8.58 (s, 1 H), 8.37 (s, 1 H), 7.83 (s, 1 H), 7.63 (d, 1 H, *J* = 7.9 Hz), 7.30 (d, 1 H, *J* = 7.8 Hz), 7.05 (t, 1 H, *J* = 7.7 Hz), 6.33 (s, 1 H), 5.81 (d, 1 H, *J* = 7.0 Hz), 5.52 (s, 2 H), 4.72–4.95 (m, 4 H), 4.36 (d, 1 H, *J* = 5.9 Hz), 2.94 (d, 3 H, *J* = 5.5 Hz), 0.78 (s, 9 H), -0.11 (s, 3 H), -0.39 (s, 3 H); IR (KBr): 3276, 2930, 1680, 1617, 1435, 1180, 1119, 723, 694 cm<sup>-1</sup>; FAB-MS *m/z* 667 [M + H]<sup>+</sup>. Anal. (C<sub>25</sub>H<sub>35</sub>-IN<sub>8</sub>O<sub>4</sub>Si) C, H, N.

**General Procedure for the Synthesis of 13, 10, 11, 14, and 12.** To a stirred solution of 30a–c and 40a,b in THF (10 mL) was added 1 M TBAF in THF (4 equiv) at room temperature. The reaction mixture was stirred for 4 h at room temperature and evaporated. The residue was purified by silica gel column chromatography to give 13, 10, 11, 14, and 12.

**N<sup>6</sup>-Methyl-9-(3-deoxy-3-ureido-β-D-ribofuranosyl)adenine (13).** 88% yield; white solid; mp 191–194 °C; [α]<sub>D</sub><sup>25</sup> -42.3° (c 0.13, DMF); <sup>1</sup>H NMR (DMSO-*d*<sub>6</sub>) δ 8.37 (s, 1 H), 8.25 (s, 1 H), 7.79 (brs, 1 H), 6.24 (s, 1 H), 6.15 (d, 1 H, *J* = 7.5 Hz), 5.91 (d, 1 H, *J* = 2.6 Hz), 5.74 (brs, 2 H), 5.13 (t, 1 H, *J* = 5.1 Hz), 4.41 (dd, 1 H, *J* = 2.6, 5.7 Hz), 4.27 (m, 1 H), 3.86 (m, 1 H), 3.68 (m, 1 H), 3.49 (dd, 1 H, *J* = 4.6, 12.5 Hz), 2.94 (s, 3 H); <sup>13</sup>C NMR (DMSO-*d*<sub>6</sub>) δ 22.6, 50.4, 60.8, 73.1, 83.1, 89.4, 119.6, 139.0, 147.9, 153.0, 155.0, 170.0; IR (KBr): 3422, 1633, 1543, 1382, 1335, 1221, 1102, 1065, 521 cm<sup>-1</sup>; FAB-MS *m/z* 324 [M + H]<sup>+</sup>. Anal. (C<sub>12</sub>H<sub>17</sub>N<sub>7</sub>O<sub>4</sub>) C, H, N.

**N<sup>6</sup>-(3-Iodobenzyl)-9-(3-deoxy-3-ureido-β-D-ribofuranosyl)adenine (10).** 70% yield; white solid; mp 165–168 °C; [α]<sub>D</sub><sup>25</sup> -43.3° (c 0.12, DMF); <sup>1</sup>H NMR (DMSO-*d*<sub>6</sub>) δ 8.44 (brs, 1 H), 8.43 (s, 1 H), 8.22 (s, 1 H), 7.71 (s, 1 H), 7.55 (d, 1 H, *J* = 7.7 Hz), 7.33 (d, 1 H, *J* = 7.9 Hz), 7.06 (t, 1 H, *J* = 7.7 Hz), 6.22 (d, 1 H, *J* = 5.0 Hz), 6.15 (d, 1 H, *J* = 7.7 Hz), 5.93 (d, 1 H, *J* = 2.3 Hz), 5.78 (brs, 2 H), 5.11 (t, 1 H, *J* = 5.7 Hz), 4.66 (brs, 2 H), 4.42 (m, 1 H), 4.25 (m, 1 H), 3.87 (m, 1 H), 3.69 (m, 1 H), 3.50 (m, 1 H); <sup>13</sup>C NMR (DMSO-*d*<sub>6</sub>) δ 42.2, 50.9, 61.0, 73.4, 84.2, 89.5, 94.7, 119.5, 126.7, 130.5, 135.4, 135.7, 139.2, 142.9, 148.3, 152.5, 154.3, 158.7; IR (KBr): 3398, 1621, 1538, 1477, 1338, 1221, 1103, 822 cm<sup>-1</sup>; FAB-MS *m/z* 526 [M + H]<sup>+</sup>. Anal. (C<sub>18</sub>H<sub>20</sub>IN<sub>7</sub>O<sub>4</sub>) C, H, N.

**{5-[2-Chloro-6-(3-iodo-benzylamino)-purin-9-yl]-4-hydroxy-2-hydroxymethyl-tetrahydro-furan-3-yl}urea (11).** 82% yield; white solid; mp 132.3–135 °C; [α]<sub>D</sub><sup>25</sup> -27.4° (c 0.35, DMF); <sup>1</sup>H NMR (DMSO-*d*<sub>6</sub>) δ 8.92 (brs, 1 H), 8.47 (s, 1 H), 7.73 (s, 1 H), 7.58 (d, 1 H, *J* = 7.9 Hz), 7.33 (d, 1 H, *J* = 7.5 Hz), 7.09 (t, 1 H, *J* = 7.7 Hz), 6.25 (d, 1 H, *J* = 4.7 Hz), 6.16 (d, 1 H, *J* = 7.7 Hz), 5.87 (d, 1 H, *J* = 2.0 Hz), 5.77 (s, 2 H), 5.05 (t, 1 H, *J* = 5.5 Hz), 4.58 (d, 2 H, *J* = 5.0 Hz), 4.34 (m, 1 H), 3.86 (m, 1 H), 3.39 (m, 1 H), 3.51 (m, 1 H); <sup>13</sup>C NMR (DMSO-*d*<sub>6</sub>) δ 42.5, 50.7, 60.7, 73.6, 84.1, 89.2, 94.7, 118.5, 126.8, 130.6, 135.6, 136.1, 139.4, 141.9, 149.3, 153.1, 154.8, 158.6; IR (KBr): 3405, 1619, 1346, 1312, 1221, 1105, 781, 633 cm<sup>-1</sup>; FAB-MS *m/z* 560 [M + H]<sup>+</sup>. Anal. (C<sub>18</sub>H<sub>19</sub>ClIN<sub>7</sub>O<sub>4</sub>) C, H, N.

**3-Ureido-5-(6-methylaminopurin-9-yl)-4-hydroxy-tetrahydro-furan-2-carboxylic Acid Methyl Amide (14).** 66% yield; white solid; mp 118.2–120.0 °C; [α]<sub>D</sub><sup>25</sup> -13.3° (c 0.15, MeOH); <sup>1</sup>H NMR (CD<sub>3</sub>OD): δ 8.48 (s, 1 H), 8.29 (s, 1 H), 6.07 (d, 1 H, *J* = 3.1 Hz), 4.61 (m, 2 H), 4.41 (d, 1 H, *J* = 6.0 Hz), 3.11 (s, 3 H), 2.80 (s, 3 H); <sup>13</sup>C NMR (CD<sub>3</sub>OD) δ 14.1, 20.9, 24.2, 24.9, 26.4, 56.7, 59.7, 74.9, 83.7, 92.2, 141.0, 154.2, 173.0; IR (KBr): 3425, 1667, 1630, 1534, 1356, 1306, 1084, 936, 636 cm<sup>-1</sup>; FAB-MS *m/z* 351 [M + H]<sup>+</sup>. Anal. (C<sub>13</sub>H<sub>18</sub>N<sub>8</sub>O<sub>4</sub>) C, H, N.

**3-Ureido-5-(6-(3-iodobenzylamino)purin-9-yl)-4-hydroxy-tetrahydro-furan-2-carboxylic Acid Methyl Amide (12).** 82% yield; white solid; mp: 120.7–122.2 °C; [α]<sub>D</sub><sup>25</sup> -10.0° (c 0.10, DMF); <sup>1</sup>H NMR (DMSO-*d*<sub>6</sub>): δ 8.69 (s, 1 H), 8.53 (brs, 1 H), 8.33 (d, 1 H, *J* = 4.6 Hz), 8.23 (s, 1 H), 7.72 (s, 1 H), 7.55 (d, 1 H, *J* = 7.7 Hz), 7.34 (d, 1 H, *J* = 7.7 Hz), 7.06 (t, 1 H, *J* = 7.7 Hz), 6.29 (d,

1 H, *J* = 4.4 Hz), 6.22 (d, 1 H, *J* = 6.7 Hz), 6.02 (d, 1 H, *J* = 2.2 Hz), 5.76 (s, 2 H), 4.65 (br s, 2 H), 4.41 (m, 2 H), 4.23 (d, 1 H, *J* = 6.0 Hz), 2.63 (d, 1 H, *J* = 4.6 Hz); <sup>13</sup>C NMR (CD<sub>3</sub>OD) δ 14.1, 20.9, 24.9, 26.4, 56.7, 59.7, 75.1, 83.6, 92.3, 128.0, 131.6, 137.5, 137.7, 141.3, 143.3, 154.2, 156.2, 161.7, 173.0; IR (KBr): 3424, 2932, 1619, 1476, 1338, 1056, 645 cm<sup>-1</sup>; FAB-MS *m/z* 553 [M + H]<sup>+</sup>. Anal. (C<sub>19</sub>H<sub>21</sub>IN<sub>8</sub>O<sub>4</sub>) C, H, N.

**Numbering Scheme of GPCRs.** For sequence alignments of selected regions of the A<sub>3</sub>AR and other GPCRs, a standardized numbering system<sup>29</sup> was used to identify residues in the TMs of various receptors. Each residue is identified by two numbers: the first corresponds to the TM in which it is located; the second indicates its position relative to the most conserved residue in that helix, arbitrarily assigned to 50. For example, Thr3.36 is the threonine in TM3 (Thr94), located 14 residues before the most conserved arginine Arg3.50; His7.43 corresponds to His272.

**Biological Methods. Materials.** The vector pcDNA3 was obtained from Invitrogen. Oligonucleotides used were synthesized by Bioserve Biotechnologies (Laurel, MD). Adenosine deaminase, 2-chloroadenosine, and NECA (5'-*N*-ethylcarboxamidoadenosine) were obtained from Sigma (St. Louis, MO). [<sup>125</sup>I]-AB-MECA (2000 Ci/mmol) was from Amersham Pharmacia Biotech (Buckinghamshire, UK). All other compounds were obtained from standard commercial sources and were of analytical grade.

**Site-directed Mutagenesis.** The protocols used were as described in the QuikChange Site-directed Mutagenesis Kit (Stratagene, La Jolla, CA). Mutations were confirmed by DNA sequencing.

**Transfection of Wild-Type and Mutant A<sub>3</sub>AR to COS-7 Cells.** Lipofectamine 2000 (Invitrogen, Carlsbad, CA) was used for transfection of wild-type and mutant receptor cDNA to COS-7 cells following the manufacturer's protocol.

**Membrane Preparation.** After 48 h of transfection, COS-7 cells were harvested and homogenized with a Polytron homogenizer. The homogenates were centrifuged at 20 000g for 20 min, and the resulting pellet was resuspended in the 50 mM Tris-HCl buffer (pH 7.4) in the presence of 3 Units/mL adenosine deaminase and incubated at 37°C for 30 min, and then stored at -80°C in aliquots. The protein concentration was determined by using the method of Bradford.<sup>30</sup>

**Radioligand Binding Assays and Inositol Phosphate Determination in COS-7 Cells.** The procedures for A<sub>3</sub>AR-binding experiments using [<sup>125</sup>I]-AB-MECA ([<sup>125</sup>I]N<sup>6</sup>-(4-aminobenzyl)-5'-*N*-methylcarboxamidoadenosine) were as previously described.<sup>41</sup> The procedures for binding at human A<sub>1</sub> and A<sub>2A</sub>ARs and a functional assay of cyclic AMP formation mediated by the human A<sub>2B</sub>AR expressed in CHO cells was as described.<sup>36</sup> The method for PLC determination in transiently transfected COS-7 cells has been previously described.<sup>31</sup>

**Preparation of Cardiac Myocyte Model of Simulated Ischemia and Gene Transfer into Cardiac Myocytes.** Ventricular cells were cultured from chick embryos 14 d in ovo and maintained in culture as previously described.<sup>27</sup> All experiments were performed on day 3 in culture, at which time the medium was changed to a HEPES (*N*-2-hydroxyethylpiperazine-*N'*-2-ethanesulfonic acid)-buffered medium containing 139 mM NaCl, 4.7 mM KCl, 0.5 mM MgCl<sub>2</sub>, 0.9 mM CaCl<sub>2</sub>, 5 mM HEPES, and 2% fetal bovine serum (pH 7.4, 37 °C). Myocytes were then exposed to simulated ischemia, which was induced by 90 min of hypoxia and glucose deprivation in a hypoxic incubator (NuAire, Plymouth, MN) where O<sub>2</sub> was replaced by N<sub>2</sub> as previously described.<sup>27</sup> The extent of myocyte injury was determined at the end of the 90-min ischemia, at which time myocytes were taken out of the hypoxic incubator and reexposed to room air (normal percentage O<sub>2</sub>), followed by quantitation of the number of viable cells. Viable cells were also determined by the ability to exclude Trypan blue.<sup>27</sup> Measurement of the basal level of cell injury was made after parallel incubation of control cells under a normal percentage of O<sub>2</sub>. The extent of ischemia-induced injury was quantitatively determined by the percentage of cells killed, according to a previously described method.<sup>27</sup> The percentage of cells killed was calculated as the

number of cells obtained from the control group (representing cells not subjected to hypoxia or drug treatment) minus the number of cells from the treatment group divided by the number of cells in the control group multiplied by 100%.

Cells were then transfected with either the vector pcDNA3 or cDNA encoding the wild-type human A<sub>3</sub>AR or the neoreceptor H272E, with the use of FuGENE 6 as previously described.<sup>28</sup> Forty-eight hours after the transfection, myocytes were exposed to simulated ischemia, and myocyte injury was determined in the presence or absence of the neoligand **10**. In other experiments, the PLD activity was determined 48 h after the transfection of myocytes with either the wild-type hA<sub>3</sub>AR or the neoreceptor H272E cDNA.

**Measurement of PLD Activity.** For measurement of PLD activity, cultured ventricular myocytes labeled with [<sup>3</sup>H]myristate (49 Ci/mmol, 2 μCi/ml) for 24 h were exposed to receptor agonist in the presence of 0.5% (v/v) ethanol. Lipids were extracted by the method of Bligh and Dyer.<sup>32</sup> The formation of [<sup>3</sup>H]PEt was an indication of PLD activity. Quantitation of PEt (phosphatidylethanol) was carried out as previously described.<sup>33</sup> Briefly, the formation of [<sup>3</sup>H]PEt in cells was quantitated by separation of the labeled lipids via thin-layer chromatography and scintillation counting of the <sup>3</sup>H label. The position of PEt was determined visually by placing the thin-layer plate in an iodine chamber, and its level was expressed as a percentage of total lipids. Data were also expressed as percentage increases in the amount of PEt relative to that for unstimulated cells.

**Statistical Analysis.** Binding and functional parameters were estimated with GraphPad Prism software (GraphPad, San Diego, CA). IC<sub>50</sub> values obtained from competition curves were converted to K<sub>i</sub> values by using the Cheng–Prusoff equation.<sup>34</sup> Data were expressed as mean ± standard error.

**Computational Methods.** All calculations were performed using the SYBYL program version 6.9<sup>53</sup> on a Silicon Graphics Octane workstation (300 MHz MIPS R12000 (IP30) processor).

**Conformational Search.** The N<sup>6</sup>-I-benzyl-3'-ureido compound, **10**, was constructed using the "Sketch Molecule" and subjected to a random search performed for all rotatable bonds. The options of the random search consisted of 3000 iterations, 3 kcal energy cutoff, and chirality checking. MMFF force field<sup>54</sup> and charge were applied using distance-dependent dielectric constants and the conjugate gradient method until the gradient reached 0.05 kcal/mol/Å. After clustering the low energy conformers from the result of the conformational search, the relative stabilities of various representative conformers from all groups were checked by semiempirical molecular orbital calculations using the PM3 method in the MOPAC 6.0 package.<sup>43</sup> During the PM3 optimization, all abortive results from electrostatic collapse were removed.

**Molecular Dynamics of the H272E Neoreceptors.** The previously published hA<sub>3</sub> AR model (PDB code: 1o74) built by homology modeling<sup>55</sup> from the X-ray structure of bovine rhodopsin with 2.8 Å resolution<sup>35</sup> was used for the docking study. For the side-chain refinement of the H272E neoreceptors, the optimized structures were then used as the starting point for subsequent 50-ps MD, during which the protein backbone atoms in the secondary structures were constrained as in the previous step. The options of MD at 300 K with a 0.2-ps coupling constant were a time step of 1 fs and a nonbonded update every 25 fs. The SHAKE algorithm<sup>56</sup> was employed to fix the lengths of bonds to hydrogen atoms. The average structure from the last 10-ps trajectory of MD was optimized with backbone constraints in the secondary structure and then the unconstrained structure was minimized as described above.

**FlexiDock Docking.** Compound **10** was docked within the hA<sub>3</sub> AR and H272E neoreceptors. Flexible docking was facilitated through the FlexiDock utility in the Biopolymer module of SYBYL 6.9. Flexible docking allowed for flexibility of all rotatable bonds in **10**, except those of the ribose ring, and the side chains of surrounding hydrophilic residues (T94, Q167, N250, E272) in the putative binding site of CI-IB-MECA. After the hydrogen atoms were added to the receptor, atomic charges were recalculated by using Kollman All-atom for the protein and Gasteiger–Hückel for

the ligand. H-bonding sites were marked for the acidic residue, E272, of the neoreceptor and for the 3'-ureido groups of the neoligands, which were able to act as H-bond donor or acceptor. The lowest energy conformer of neoligand was variously prepositioned in the putative binding cavity as a starting point for FlexiDock, based on the reported point-mutational results. FlexiDock parameters were set at 30 000-generation for genetic algorithms. To increase the binding interaction, the torsion angles of the side chains that directly interacted within 5 Å of the ligands, according to the results of FlexiDock, were manually adjusted. The atom types of all ligands were manually assigned with an Amber all-atom force field. Finally, the complex structure was minimized using an Amber force field with a fixed dielectric constant (4.0), until the conjugate gradient reached 0.1 kcal·mol<sup>-1</sup>·Å<sup>-1</sup>.

**FlexX Docking.** FlexX 1.13<sup>57</sup> is a fast docking method that uses a new algorithmic approach based on a pattern recognition technique called pose clustering, allowing conformational flexibility of the ligand by MINUMBA<sup>58</sup> conformer library to grow ligands during the docking process. The free binding energy of complex including H-bond, ionic, aromatic, or lipophilic interactions was estimated by the scoring function. Cscore calculations were included for scoring. A putative binding site including T94 (3.36), N250 (6.55), S271 (7.42), and H272 (7.43) was manually selected, based on the previous point-mutational results.<sup>41</sup> Formal charges were applied to the ligands. All default parameters, as implemented in the 6.9 release of SYBYL, were used.

**Acknowledgment.** We thank Dr. Michihiro Ohno for helpful discussion. This research was supported by a grant from the Korea Science and Engineering Foundation (R01-2005-000-10162-0). Dr. Philippe Van Rompaey is a recipient of an IWT fellowship. This research was supported in part by the Intramural Research Program of the NIH, National Institute of Diabetes and Digestive and Kidney Diseases, and R01-HL48225 to BTL.

**Supporting Information Available:** Elemental analysis data for unknown compounds and 3D coordinates of two modes of docking compound **10** in homology models of the H272E mutant human A<sub>3</sub> receptors in PDB format (as represented in Figure 3). This material is available free of charge via the Internet at <http://pubs.acs.org>.

## References

- (1) Buskirk, A. R.; Liu, D. R. Creating small-molecule-dependent switches to modulate biological functions. *Chem. Biol.* **2005**, *12*, 151–161.
- (2) Hwang, Y. W.; Miller, D. L. A mutation that alters the nucleotide specificity of elongation factor Tu, a GTP regulatory protein. *J. Biol. Chem.* **1987**, *262*, 13081–13085.
- (3) Niculescu-Duvaz, I.; Friedlos, F.; Niculescu-Duvaz, D.; Davies, L.; Springer, C. J. Prodrugs for antibody- and gene-directed enzyme prodrug therapies (ADEPT and GDEPT). *Anticancer Drug Des.* **1999**, *14*, 517–538.
- (4) Hashimoto, A.; Shi, Y.; Drake, K.; Koh, J. T. Design and synthesis of complementing ligands for mutant thyroid hormone receptor TRbeta(R320H): a tailor-made approach toward the treatment of resistance to thyroid hormone. *Bioorg. Med. Chem.* **2005**, *13*, 3627–3639.
- (5) Strausberg, R. L.; Schreiber, S. L. From knowing to controlling: a path from genomics to drugs using small molecule probes. *Science* **2003**, *300*, 294–295.
- (6) Koh, J. T.; Biggins, J. B. Ligand–receptor engineering and its application towards the complementation of genetic disease and target identification. *Curr. Top. Med. Chem.* **2005**, *5*, 413–420.
- (7) Shi, Y.; Koh, J. T. Functionally orthogonal ligand–receptor pairs for the selective regulation of gene expression generated by manipulation of charged residues at the ligand–receptor interface of ER alpha and ER beta. *J. Am. Chem. Soc.* **2002**, *124*, 6921–6928.
- (8) Tedesco, R.; Thomas, J. A.; Katzenellenbogen, B. S.; Katzenellenbogen, J. A. The estrogen receptor: a structure-based approach to the design of new specific hormone-receptor combinations. *Chem. Biol.* **2001**, *8*, 277–287.
- (9) Liu, Y.; Shah, K.; Yang, F.; Witucki, L.; Shokat, K. M. Engineering Src family protein kinases with unnatural nucleotide specificity. *Chem. Biol.* **1998**, *5*, 91–101.

- (10) Lin, Q.; Jiang, F.; Schultz, P. G.; Gray, N. S. Design of allele-specific protein methyltransferase inhibitors. *J. Am. Chem. Soc.* **2001**, *123*, 11608–11613.
- (11) Strader, C. D.; Sigal, I. S.; Register, R. B.; Candelore, M. R.; Rands, E.; Dixon, R. A. Identification of residues required for ligand binding to the beta-adrenergic receptor. *Proc. Natl. Acad. Sci. U.S.A.* **1987**, *84*, 4384–4388.
- (12) Strader, C. D.; Gaffney, T.; Sugg, E. E.; Candelore, M. R.; Keys, R.; Patchett, A. A.; Dixon, R. A. Allele-specific activation of genetically engineered receptors. *J. Biol. Chem.* **1991**, *266*, 5–8.
- (13) Small, K. M.; Wagoner, L. E.; Levin, A. M.; Kardia, S. L.; Liggett, S. B. Synergistic polymorphisms of beta1- and alpha2C-adrenergic receptors and the risk of congestive heart failure. *N. Engl. J. Med.* **2002**, *347*, 1135–1142.
- (14) Coward, P.; Wada, H. G.; Falk, M. S.; Chan, S. D.; Meng, F.; Akil, H.; Conklin, B. R. Controlling signaling with a specifically designed Gi-coupled receptor. *Proc. Natl. Acad. Sci. U.S.A.* **1998**, *95*, 352–357.
- (15) Redfern, C. H.; Coward, P.; Degtyarev, M. Y.; Lee, E. K.; Kwa, A. T.; Hennighausen, L.; Bujard, H.; Fishman, G. I.; Conklin, B. R. Conditional expression and signaling of a specifically designed Gi-coupled receptor in transgenic mice. *Nat. Biotechnol.* **1999**, *17*, 165–169.
- (16) Scarce-Lavie, K.; Lieberman, M. D.; Elliott, H. H.; Conklin, B. R. Engineered G protein coupled receptors reveal independent regulation of internalization, desensitization and acute signaling. *BMC Biol.* **2005**, *3*, 3.
- (17) Claeysen, S.; Joubert, L.; Sebben, M.; Bockaert, J.; Dumuis, A. A single mutation in the 5-HT<sub>4</sub> receptor (5-HT<sub>4</sub>-R D100(3.32)A) generates a Gs-coupled receptor activated exclusively by synthetic ligands (RASSL). *J. Biol. Chem.* **2003**, *278*, 699–702.
- (18) Pauwels, P. J. Unravelling multiple ligand-activation binding sites using RASSL receptors. *Trends Pharmacol. Sci.* **2003**, *24*, 504–507.
- (19) Zhao, G. Q.; Zhang, Y.; Hoon, M. A.; Chandrasekar, J.; Erlenbach, I.; Ryba, N. J.; Zuker, C. S. The receptors for mammalian sweet and umami taste. *Cell* **2003**, *115*, 255–266.
- (20) Bruyters, M.; Jongejan, A.; Akdemir, A.; Bakker, R. A.; Leurs, R. Mutant histamine H<sub>1</sub> receptor Phe435Ala: A Gq/11-coupled receptor activated solely by synthetic ligands (RASSL). *J. Biol. Chem.* **2005**, Jul 18; [Epub ahead of print].
- (21) Jacobson, K. A.; Gao, Z. G.; Chen, A.; Barak, D.; Kim, S. A.; Lee, K.; Link, A.; Van Rompaey, P.; Van Calenbergh, S.; Liang, B. T. Neoreceptor concept based on molecular complementarity in GPCRs: A mutant adenosine A<sub>3</sub> receptor with selectively enhanced affinity for amine-modified nucleosides. *J. Med. Chem.* **2001**, *44*, 4125–4136.
- (22) Liang, B. T.; Jacobson, K. A. A physiological role of the adenosine A<sub>3</sub> receptor: sustained cardioprotection. *Proc. Natl. Acad. Sci. U.S.A.* **1998**, *95*, 6995–6999.
- (23) Fredholm, B. B.; Chen, J. F.; Masino, S. A.; Vaugeois, J. M. Actions of adenosine at its receptors in the CNS: insights from knockouts and drugs. *Annu. Rev. Pharmacol. Toxicol.* **2005**, *45*, 385–412.
- (24) Fishman, P.; Bar-Yehuda, S.; Madi, L.; Cohn, I. A<sub>3</sub> adenosine receptor as a target for cancer therapy. *Anticancer Drugs* **2002**, *13*, 437–443.
- (25) Kim, S. K.; Gao, Z. G.; Van Rompaey, P.; Gross, A. S.; Chen, A.; Van Calenbergh, S.; Jacobson, K. A. Modeling the adenosine receptors: Comparison of binding domains of A<sub>2A</sub> agonist and antagonist. *J. Med. Chem.* **2003**, *46*, 4847–4859.
- (26) Jacobson, K. A.; Ohno, M.; Duong, H. T.; Kim, S. K.; Tchilibon, S.; Cesnek, M.; Holy, A.; Gao, Z. G. A neoreceptor approach to unraveling microscopic interactions between the human A<sub>2A</sub> adenosine receptor and its agonists. *Chem. Biol.* **2005**, *12*, 237–247.
- (27) Strickler, J.; Jacobson, K. A.; Liang, B. T. Direct preconditioning of cultured chick ventricular myocytes: novel functions of cardiac adenosine A<sub>2A</sub> and A<sub>3</sub> receptors. *J. Clin. Invest.* **1996**, *98*, 1773–1779.
- (28) Mozzicato, S.; Joshi, B. V.; Jacobson, K. A.; Liang, B. T. Role of direct RhoA-phospholipase D interaction in mediating adenosine-induced protection from cardiac ischemia. *FASEB J.* **2004**, *18*, 406–408.
- (29) Visiers, I.; Ballesteros, J. A.; Weinstein, H. Three-dimensional representations of G protein-coupled receptor structures and mechanisms. *Methods Enzymol.* **2002**, *343*, 329–371.
- (30) Bradford, M. M. A rapid and sensitive method for the quantitation of microgram quantities of protein utilizing the principle of protein-dye binding. *Anal. Biochem.* **1976**, *72*, 248–254.
- (31) Gao, Z. G.; Chen, A.; Barak, D.; Kim, S. K.; Müller, C. E.; Jacobson, K. A. Identification by site-directed mutagenesis of residues involved in ligand recognition and activation of the human A<sub>3</sub> adenosine receptor. *J. Biol. Chem.* **2002**, *277*, 19056–19063.
- (32) Bligh, E. G.; Dyer, W. J. A rapid method of total lipid extraction and purification. *Can. J. Biochem. Physiol.* **1959**, *37*, 911–917.
- (33) Lee, J. E.; Bokoch, G.; Liang, B. T. Signaling mechanism of the adenosine A<sub>3</sub> receptor: Novel cardioprotective role of RhoA. *FASEB J.* **2001**, *15*, 1886–1894.
- (34) Cheng, Y.; Prusoff, W. H. Relationship between the inhibition constant (K<sub>i</sub>) and the concentration of inhibitor which causes 50% inhibition (I<sub>50</sub>) of an enzymatic reaction. *Biochem. Pharmacol.* **1973**, *22*, 3099–3108.
- (35) Palczewski, K.; Kumasaka, T.; Hori, T.; Behnke, C. A.; Motoshima, H.; Fox, B. A.; Le Trong, I.; Teller, D. C.; Okada, T.; Stenkamp, T. E.; Yamamoto, M.; Miyano, M. Crystal structure of rhodopsin: a G protein-coupled receptor. *Science* **2000**, *289*, 739–745.
- (36) Ohno, M.; Gao, Z. G.; Van Rompaey, P.; Tchilibon, S.; Kim, S. K.; Harris, B. A.; Blaustein, J.; Gross, A. S.; Duong, H. T.; Van Calenbergh, S.; Jacobson, K. A. Modulation of adenosine receptor affinity and intrinsic efficacy in nucleosides substituted at the 2-position. *Bioorg. Med. Chem.* **2004**, *12*, 2995–3007.
- (37) Van Rompaey, P.; Jacobson, K. A.; Gross, A. S.; Gao, Z. G.; Van Calenbergh, S. Exploring human adenosine A<sub>3</sub> receptor complementarity and activity for adenosine analogues modified in the ribose and purine moiety. *Bioorg. Med. Chem.* **2005**, *13*, 973–983.
- (38) Jeong, L. S.; Kim, M. J.; Kim, H. O.; Kim, S. K.; Gao, Z. G.; Jacobson, K. A.; Chun, M. W. Design and synthesis of 3'-ureidoadenosine-5'-uronamides: Effects of the 3'-ureido group on binding to the A<sub>3</sub> adenosine receptor. *Bioorg. Med. Chem. Lett.* **2004**, *14*, 4851–4854.
- (39) Jeong, L. S.; Kim, M. J.; Kim, A. Y.; Lee, J. A.; Jacobson, K. A.; Gao, Z. G.; Kim, S. K.; Chun, M. W. Presented at the 229th National Meeting of the American Chemical Society, Abstract MEDI82, San Diego, CA, March 13–17, 2005.
- (40) Dougherty, C.; Barucha, J.; Schofield, P.; Jacobson, K. A.; Liang, B. T. Cardiac myocytes rendered ischemia resistant by overexpressing the human adenosine A<sub>3</sub> receptor. *FASEB J.* **1998**, *12*, 1785–1792.
- (41) Gao, Z. G.; Kim, S. K.; Gross, A. S.; Chen, A.; Blaustein, J.; Jacobson, K. A. Identification of essential residues involved in the allosteric modulation of the human A<sub>3</sub> adenosine receptor. *Mol. Pharmacol.* **2003**, *63*, 1021–1031.
- (42) Costanzi, S.; Lambertucci, C.; Vittori, S.; Volpini, R.; Cristalli, G. 2- and 8-alkynyladenosines: conformational studies and docking to human adenosine A<sub>3</sub> receptor can explain their different biological behavior. *J. Mol. Graphics Modell.* **2003**, *21*, 253–262.
- (43) Stewart, J. J. P. MOPAC: A Semiempirical Molecular Orbital Program. *J. Comput.-Aided Mol. Des.* **1990**, *4*, 1–105.
- (44) Spiegel, A. M.; Weinstein, L. S. Inherited diseases involving G proteins and G protein-coupled receptors. *Annu. Rev. Med.* **2004**, *55*, 27–39.
- (45) Iida, A.; Saito, S.; Sekine, A.; Kataoka, Y.; Tabei, W.; Nakamura, Y. Catalog of 300 SNPs in 23 genes encoding G-protein coupled receptors. *J. Hum. Genet.* **2004**, *49*, 194–208.
- (46) Lam, P.; Hong, C. J.; Tsai, S. J. Association study of A<sub>2A</sub> adenosine receptor genetic polymorphism in panic disorder. *Neurosci. Lett.* **2005**, *378*, 98–101.
- (47) Alsene, K.; Deckert, J.; Sand, P.; de Wit, H. Association between A<sub>2A</sub> receptor gene polymorphisms and caffeine-induced anxiety. *Neuropsychopharmacology* **2003**, *28*, 1694–702.
- (48) Koh, J. T. Designing selectivity and discrimination into re-engineered ligand–receptor interfaces; Beyond bumps and holes. *Chem. Biol.* **2002**, *9*, 17–23.
- (49) Belshaw, P. J.; Schoepfer, J. G.; Liu, K.-Q.; Morrison, K. L.; Schreiber, S. L. Rational design of orthogonal receptor ligand combinations. *Angew. Chem., Int. Ed. Engl.* **1995**, *34*, 2129–2132.
- (50) Gillespie, P. G.; Gillespie, S. K.; Mercer, J. A.; Shah, K.; Shokat, K. M. Engineering of the myosin- $\beta$  nucleotide-binding pocket to create selective sensitivity to N<sup>6</sup>-modified ADP analogs. *J. Biol. Chem.* **1999**, *274*, 31373–31381.
- (51) Ulrich, S. M.; Buzko, O.; Shah, K.; Shokat, K. M. Towards the engineering of an orthogonal protein kinase/nucleotide triphosphate pair. *Tetrahedron* **2000**, *56*, 9495–9502.
- (52) Fredholm, B. B.; IJzerman, A. P.; Jacobson, K. A.; Klotz, K. N.; Linden, J. International Union of Pharmacology. XXV. Nomenclature and classification of adenosine receptors. *Pharmacol. Rev.* **2001**, *53*, 527–552.
- (53) Sybyl Molecular Modeling System, version 6.9; Tripos Inc., St. Louis, MO 63144.
- (54) Halgren, T. A. MMFF VII. Characterization of MMFF94s, MMFF94s, and Other Widely Available Force Fields for Conformational Energies and for Intermolecular-Interaction Energies and Geometries. *J. Comput. Chem.* **1999**, *20*, 730–748.

- (55) Gao, Z.-G.; Kim, S.-K.; Biadatti, T.; Chen, W.; Lee, K.; Barak, D.; Kim, S. G.; Johnson, C. R.; Jacobson, K. A. Structural Determination of A<sub>3</sub> Adenosine Receptor Activation: Nucleoside Ligands at the Agonist/Antagonist Boundary. *J. Med. Chem.* **2002**, *45*, 4471–4484.
- (56) Ryckaert, J. P.; Ciccotti, G.; Berendsen, H. J. C. Numerical Integration of the Cartesian Equations of Motion for a System with Constraints: Molecular Dynamics of *n*-alkanes. *J. Comput. Phys.* **1977**, *23*, 327–341.
- (57) Rarey, M.; Kramer, B.; Lengauer, T.; Klebe, G. A fast flexible docking method using an incremental construction algorithm. *J. Mol. Biol.* **1996**, *261*, 470–489.
- (58) Klebe, G.; Mietzner, T. A fast and efficient method to generate biologically relevant conformations. *J. Comput.-Aided Mol. Des.* **1994**, *8*, 583–606.

JM050968B